Nina Sasaki Støa-Aanensen

AIR LOAD BREAK SWITCH DESIGN PARAMETERS

Thesis for the degree of Philosophiae Doctor

Trondheim, October 2015

Norwegian University of Science and Technology
Faculty of Information Technology,
Mathematics and Electrical Engineering
Department of Electric Power Engineering

NTNU
Norwegian University of
Science and Technology

NTNU
Norwegian University of Science and Technology

Thesis for the degree of Philosophiae Doctor

Faculty of Information Technology, Mathematics and Electrical Engineering
Department of Electric Power Engineering

© Nina Sasaki Støa-Aanensen

ISBN 978-82-326-1160-7 (print)
ISBN 978-82-326-1161-4 (digital)
ISSN 1503-8181

Doctoral theses at NTNU, 2015:252

Printed by NTNU Grafisk senter

Abstract

Current interruption is vital in the power system, as this makes it possible to control the use of different loads, change the grid configuration, and minimize damage when faults occur. This thesis presents a study of the different switch design and test circuit parameters involved in medium voltage air load break switching and how they affect the thermal interrupting capability. Medium-voltage load break switches are common in the distribution grid, and are a cheaper option than installing circuit breakers.

Medium voltage load current ratings are typically in the range of 6 – 36 kV and 400 A up to around 1 kA (50 Hz). Air is considered an environmentally benign alternative as an interrupting medium compared to SF_6 for these ratings, and is also thought to be cost-competitive compared to vacuum. However, no compact air load break switch for 24 kV is currently available for commercial use. Thus, it is necessary to have a good understanding of the design parameters involved, and how they affect the interrupting capability of the switch.

This thesis addresses medium-voltage load current interruption in air. It is an empirical study based on an extensive test program in a medium voltage test lab, and the main results and contents of this thesis are presented in five papers. The two first are switch design parameter studies. Using a test switch that is simple and axisymmetric, yet in many aspects similar to commercial puffer devices, one test switch parameter has been changed at a time to find the air flow over-pressure needed for successful interruption. The test circuit settings are also varied to find how the interrupting capability changes with load currents in the range 400 – 880 A, and with a transient recovery voltage corresponding to IEC's 24 kV "mainly active load" test duty. Only the thermal phase of current interruption has been considered, i.e. the first tens of microseconds after current zero. The over-pressures needed to interrupt the load currents were typically from 0.2 to 0.4 bar.

The third paper presents a logistic regression analysis of all the conducted interruption tests, with the goal of describing the interruption performance as a function of the main test switch design parameters and transient recovery voltage stresses. More than 3 000 interruption tests are used as input data for this analysis, which produce a mathematical expression that summarizes all the empirical results.

The nozzle-to-contact diameter ratio has been found to be an important design factor. Low ratios require a substantially lower air over-pressure than high nozzle-to-contact diameter ratios in order to interrupt successfully. The choice of contact diameter important as well, where larger contact diameters require lower over-pressures, but higher mass flow rates. The nozzle length does not influence the interrupting capability very much, but the chance of successful

interruption is greater when the pin contact has moved out of the nozzle at current zero. The interruption becomes more difficult with increasing current and the rate of the voltage build-up across the contacts after interruption.

The other two papers are based on the current interruption experiments mentioned above, but concern details of the arc behavior and arc voltage under different currents, test design variations and air flow conditions. For typical medium-voltage and load current ratings, the arc greatly affects the air flow during current interruption. The flow through the tulip contact and nozzle is clogged during the high current part of the half-cycle, even for moderate currents and relatively large contact dimensions. The typical over-pressures needed for successful interruption correspond to air velocities that are well below supersonic level. The arc voltage is a function of several parameters, and rises with increasing air over-pressure, decreasing current, and a larger contact gap. There is also a clear visible difference in the arc appearance when it is either subjected to forced cooling or not. The typical arc voltage is a few hundred volts.

Preface

The work on this thesis was carried out in the period between September 2011 and April 2015. It is submitted as a paper collection, partially fulfilling the requirements for the degree of philosophiae doctor (PhD) in Electric Power Engineering at the Norwegian University of Science and Technology, NTNU. This work has been supported by the Research Council of Norway, and is a part of a research project in collaboration with SINTEF Energy Research and ABB.

Chief Scientist Magne Runde has been the main supervisor for this work, with Professor Arne Nysveen as co-supervisor.

Acknowledgments

I want to thank Magne Runde for all the support during these four years, both with the scientific parts of the work, all advice and help during the writing of the papers, and with keeping my psyche above a critical level. It seems like your rare combination of being patient, yet a bit restless, is a good quality in a supervisor.

I also want to thank Erik Jonsson. In addition to building the laboratory setup, you have been a great lab and discussion partner. This work would have been much lonelier (and less fun) without you.

I also give grateful thanks to Arne Nysveen, Magne Saxegaard, Erland Strendo, Anders Dall'Osso Teigset and Elham Attar, and everyone else who have helped me during this work.

Finally, I want to thank Bendik Støa-Aanensen (the cause of the confusing name changing in the papers), who is the main reason that I have managed to stay sane during this sometimes stressful period, and my two families, KTMAA and PESKL.

List of Publications and Contributions From Individual Authors

I. Erik Jonsson, Nina Sasaki Aanensen, and Magne Runde, *Current Interruption in Air for a Medium-Voltage Load Break Switch*, IEEE Transactions on Power Delivery, vol. 29, no. 2, February 2014.

Erik Jonsson planned the experimental setup, carried out the experiments, and wrote the paper. Nina Sasaki Aanensen carried out the experiments and contributed in the discussions of the results. Magne Runde contributed in the discussions of the results and with the writing of the paper.

II. Nina Sasaki Aanensen, Erik Jonsson, and Magne Runde, *Air-Flow Investigation for a Medium-Voltage Load Break Switch*, IEEE Transactions on Power Delivery, vol. 30, no.1, January 2015.

Nina Sasaki Aanensen planned the experimental setup, carried out the experiments and computational simulations, and wrote the paper. Erik Jonsson assisted with the experimental setup and contributed in the discussions of the results. Magne Runde contributed in the discussions of the results and with the writing of the paper.

III. Nina Sasaki Støa-Aanensen, Magne Runde, Erik Jonsson, and Anders Dall'Osso Teigset, *Empirical Relationships Between Load Break Switch Parameters and Interruption Performance*, submitted to IEEE Transactions on Power Delivery.

Nina Sasaki Støa-Aanensen carried out the experiments, performed the regression analysis, and wrote the paper. Magne Runde contributed in the discussions of the results and with the writing of the paper. Erik Jonsson and Anders Dall'Osso Teigset carried out parts the experimental work.

IV. Nina Sasaki Støa-Aanensen and Magne Runde, *Air Flow Measurements During MV Load Current Interruptions*, accepted to Symposium on Physics of Switching Arc and accepted for publication in Plasma Physics and Technology, September 2015.

Nina Sasaki Støa-Aanensen planned the experimental setup, carried out the experiments and numerical calculations, and wrote the paper. Magne Runde contributed in the discussions of the results and with the writing of the paper.

V. Nina Sasaki Støa-Aanensen, Magne Runde, and Anders Dall'Osso Teigset, *Arcing Voltage for a Medium-Voltage Air Load Break Switch*, submitted to IEEE Holm Conference on Electrical Contacts, October 2015.

Nina Sasaki Støa-Aanensen planned the experimental setup, carried out the experiments, and wrote the paper. Magne Runde contributed in the discussions of the results and with the writing of the paper. Anders Dall'Osso Teigset carried out the experiments and contributed in the discussions of the results.

Contents

Chapter 1

Introduction

Devices for making and breaking the electric current are vital to our electric power system. These components are typically referred to as switchgear, switches, or breakers. They are integral components in the generation, transmission, and distribution part of the grid. Hence, their ratings and requirements vary considerably.

For load current interruption in medium-voltage (MV) distribution systems, the voltage is typically in the range 6 – 36 kV and currents are up to around 1 kA. Load break switches (LBSs) are widely used in the distribution network, often as a component in compact metal-enclosed substations, and in series with a fuse, which interrupts fault currents.

Today, most of such compact metal-enclosed switchgear is filled with sulfur hexafluoride (SF_6). However, due to the increasing effort to reduce the use of this extremely potent greenhouse gas, switchgear manufacturers are looking for alternative solutions. One option is to use air as the interrupting and insulating medium.

When the contacts in a load break switch separate, an electric arc is created. The arc continues to carry the current through a plasma created by metal vapor from the contacts and the gas (the air or SF_6) in the contact gap. To successfully interrupt the current, other measures in addition to just separating the contacts are required, such as applying forced cooling of the arc. If there is sufficient cooling, the current is interrupted at its natural current zero crossing.

Air has been used as interrupting medium in both low and high voltage switchgear for many decades. However, air is a poorer interrupting medium and only has about a third of SF_6's dielectric strength, the problem is to make air-filled switchgear as compact as today's SF_6 solutions. Most metal-enclosed switchgear is placed in space-tight rooms or in small indoor substations, and new equipment should not exceed the size of older units. Consequently, there are challenges regarding both the dielectric design of the switchgear, and the arc quenching and current interruption capability. This thesis addresses the latter.

In order to successfully design and develop cost-competitive and compact MV air LBSs, a thorough understanding of the current interruption process for the relevant ratings must be obtained. The main objective of the present work is determining which design parameters are most important, and how they influence the interrupting capability.

The air flow used to cool and quench the arc is an important part of the

interruption process. Investigations have been carried out with the purpose of finding out more about the air flow and arc interaction, in particular to find out to what extent the arc affects the air flow during the interruption.

There is little published research on MV load current interruption in air. Various topics related to high-voltage circuit breakers rated for breaking short-circuit currents of several tens of kiloamperes at up to several hundred kilovolts have received far more attention in the literature. Moreover, performing full-scale experimental current switching tests is costly, both in terms of time and money, and requires specialized, dedicated laboratory facilities. Another reason is that the development of new MV LBSs is mainly done by the switchgear manufacturers, who do not want to share sensitive information about their new products, and do not necessarily perform extensive and systematic parameter studies.

The present work is mainly experimental, using a MV test circuit powered directly from the grid and based on the standard issued by IEC. A simple, axisymmetric generic test switch has been used, where most design parameters, such as contact size, air flow over-pressure, nozzle dimensions, and contact movement can be controlled and changed independently. The goal has been to establish empirical relationships between the different design parameters and the interrupting performance under different switching conditions (currents and recovery voltages). Several thousand interruption tests were carried out during the course of this work. In addition, some simple air flow simulations using a commercial software package are performed to support the interpretation of the experimental results.

The structure of the thesis is as follows: First, there is an introduction to current interruption technology and a short overview of existing literature is given. Then, a description of the experimental setup and scope of work is presented in Chapter 3. In Chapter 4, some examples showing the possible outcomes of a current interruption attempt are given before the main work consisting of five papers is presented. The final chapter contains the conclusions based on the present results, together with suggestions for further work.

Chapter 2

Background and Scope of Work

When the contacts in a gas-filled MV LBS separate, an arc is ignited. The arc is a hot plasma consisting of neutral particles and conducting ions and electrons, made by heating the gas and contact material to several thousand degrees Kelvin by the flowing current. The current simply continues to flow from one contact to the other, through this plasma channel. In order to extinguish the arc and interrupt the current, other measures than just separating the contacts are needed. One solution is to blow cold gas onto the arc to reduce its temperature and thus also its electrical conductivity. The gas can be blown along the axis of the arc, radially onto the arc, or both (simultaneously). For moderate ratings, such as the MV level, axially blown arcs are the most common. A typical gas breaker consists of two arcing contacts, often a pin/tulip contact pair, with a nozzle in an insulating material to guide the gas flow. The flow is often generated using a so-called puffer device, where a piston linked to the contact movement is used to compress a gas volume during contact separation.

An ideal gas for use in current interruption can be characterized by being a perfect conductor from the moment the contacts separate until the current reaches its natural current zero (CZ) crossing. At that point, it should become a perfect insulator, thus interrupting the current. In reality, no gas is able to change its properties instantaneously, and the conductivity at high temperatures and dielectric strength at low temperatures vary considerably from gas to gas. The dielectric strength rises with increasing gas pressure.

As pointed out earlier, there is little published literature on load break switching at MV. Moreover, after the development of SF_6 puffer-based switchgear (and vacuum interrupters), air has been of less interest to manufacturers and researchers. Still, publications on current interruption using puffer-type devices could be of interest and be relevant to this work, even though other gases are used and voltage and current ratings are much higher.

Before 1960 – 1970, the two dominating high-voltage circuit breaker technologies were minimum oil and air blast breakers. These were reliable and robust (some are still in operation today), but they require a lot of maintenance and the air blast breakers were noisy. In the 1960s and 1970s, SF_6 started to take over for air and oil as the interrupting medium, with its remarkable arc

quenching abilities and good dielectric strength. First, the air was more or less replaced by SF_6-gas in the gas blast breakers, where the gas in a separate compartment is pumped up to a high over-pressure (usually tens of bar) and released by opening a valve to provide a gas blast onto the arc during current interruption. Later, so-called single pressure or puffer-type SF_6 circuit breakers were developed, where the gas compression is made by a piston and the movement of the contact.

There are numerous publications on gas blast breakers from this period, with both theoretical and experimental investigations, e.g., [1] – [7]. Most of these are focused on experiments with high currents up to 50 – 60 kA. Interruption tests with both air and SF_6 as the interrupting medium are carried out, with pressures in the range 4 – 50 bar. These are extremely high pressures, and well above the over-pressures needed for successful interruption in the cases reported in the present work, which are typically below 1 bar over-pressure.

During the 1980s, more refined SF_6 circuit breakers exploiting the so-called "self-blast" effects were developed, where the pressure build-up from the arc itself during the high current part of the half-cycle is used to cool the arc during the low current part. The "self-blast" principle can be used by itself, or in a combination with a puffer device. Another technology that was developed and became increasingly popular during the 1980s was the vacuum breakers, where the arc burns in the metal vapor of the arcing contacts. Vacuum and SF_6 technology became totally dominating during the following years for high-voltage circuit breakers, with vacuum and SF_6 being used for the lower voltage ratings (up to approximately 72 kV) and SF_6 for higher voltages.

Today, SF_6-based circuit breakers are considered a mature technology. Much optimization has been done to make the devices cheaper, smaller, and requiring less driving force and maintenance, but the basic design of the puffer device is the same. During the last couple of decades, advanced computational models have been developed to bring theoretical and experimental knowledge closer together. Recent publications are often focused on such numerical calculations, where the results are compared and verified by real measurements (e.g., the works mentioned above). With the development of advanced computational fluid dynamic or multi-physics models, more detailed knowledge and understanding of the arc and current interruption process have been obtained. For example, models that are able to predict the amount and nature of the turbulent mixing of the plasma and the interrupting gas, which is directly connected to the cooling efficiency, are being developed.

Presently, several research groups work with numerical investigations on current interruption, e.g., at the ABB research center in Baden [8] – [11], the University of Liverpool [12] – [14], and also elsewhere [15] – [18]. Again, most of this work concerns interruption of large short-circuit currents at several hundred kilovolts, i.e., ratings for high-voltage circuit breakers. An attempt to apply computational models for such ratings on lower energy puffer-based interrupters is reported in [19].

After the Kyoto protocol of 1997 stated that SF_6 is among the most potent greenhouse gases known, its use and release have been regulated and attempts have been made to reduce it. The motivation for developing SF_6-free switchgear is increasing, and more research on alternative interrupting gases is being published. Air is an obvious choice with respect to environmental aspects, but is not a competitive option for replacing SF_6 at the highest voltage ratings and for

fault currents. Another candidate is CO_2, which has shown promising current interrupting properties [21]. Different gas mixes have also been investigated, such as gases containing fluorine mixed with e.g. CO_2 or air [22] – [25]. A study by Morita treats the development of switchgear in the distribution system in Japan, with several SF_6-free alternatives, of which one is air-based [20].

Since no known gas has a similarly excellent current interrupting performance combined with good dielectric strength as SF_6, the first application areas for other gases and new technology are believed to be in applications with more moderate voltage and current levels, such as MV LBS ratings. When using SF_6, interrupting load currents is quite simple, and many of the puffer devices used in SF_6 LBSs are simplified and down-scaled versions of circuit breaker design, and not necessarily optimized with regard to design and cost. If air is to replace SF_6 in MV LBSs, more research that specifically addresses designs for load current and medium-voltage level is needed. Simply increasing the air pressure to compensate for the poorer properties is not an option, as these products are filled and "sealed for life" at the factory before being shipped to its installation site. Safety concerns and cost of shipping set a limit on the gas pressure in the metal-enclosed switchgear to 1.3 bar.

Moreover, the main challenge is believed to be the thermal phase of the current interruption. Without being able to interrupt the current in the critical period around CZ, good dielectric strength in the other parts of the switchgear becomes irrelevant.

For further reading on current interruption, switchgear, and the properties of interrupting medium see textbooks, such as [26] – [28].

2.1 Scope of Work

This thesis work is an empirical and experimental study of the different parameters relevant to an MV air LBS application. It is a continuation of the work presented in [29] (see also [30] – [34]), with the main focus being on identifying which design parameters that are most decisive for making an optimized LBS with air as the interrupting medium. The test switch that has been used is based on the same principle as commercial puffer devices, where an upstream over-pressure drives the air flow used to cool the arc. In the test switch, however, the puffer device is replaced with a pressure tank. The tank can be pre-set to a certain upstream over-pressure, and the tank is large enough to keep this over-pressure during the entire interruption test. In commercial puffer devices, the contact movement is directly linked to the pressure build-up and flow.

By using this simple, idealized switch, the effect of various design parameters on the performance can be more easily identified. The range of parameters considered in this work are:

- A transient recovery voltage (TRV) corresponding to the thermal phase of the 24 kV class of IEC's "mainly active load" test duty (70 – 73 V/μs) [35]. (In the regression analysis, interruption tests from [32] with a wider range of the TRV are included.)

- Currents in the range of 400 to 880 A, with a frequency of 50 Hz. (Again, the regression analysis includes interruption tests from [32] with currents from 300 A to 900 A.)

- Polytetrafluoroethylene (PTFE) nozzles with lengths between 10 and 60 mm, and inner diameters between 4.2 and 13.6 mm.
- Arcing pin contacts with diameters in the range 3 to 10 mm.
- Different pin contact positions, i.e. different contact gaps, at CZ.
- A moving pin contact speed of 5 ± 0.5 m/s.
- Surrounding air at atmospheric pressure, and tank over-pressures up to 1.4 bar.

Considering the combinations of these parameters, the goal has been to:

- Find the required upstream over-pressure required for successful thermal interruption.
- Establish quantitative relationships between the different parameters and interrupting capability.
- Increase the understanding about the arc and the arc / air flow interaction, by investigating the arc voltage, air flow pressures during interruption and imaging the arc behavior with a high-speed camera.

The work does not include:

- Studies of the effect of different nozzle and contact materials, such as the use of ablation materials.
- Computational simulations of the current interruption process or detailed theoretical descriptions of the arc and the plasma in which it burns.
- Investigations concerning the dielectric phase of current interruption, as this is considered a less difficult task than interrupting the thermal phase.

Chapter 3

Experimental Setup

This chapter contains a short description of the test setup that has been used for all the experimental work.

3.1 Test Circuit

Fig. 3.1 presents the laboratory test circuit. It is directly powered from the 11.4 kV distribution grid in Trondheim, which is further transformed to a system voltage of 13.8 kV by a laboratory transformer. The test circuit is similar to a single-phase version of the "mainly active load" test duty as described in [35], with a parallel resistive/inductive load (R_l and L_l). The system side is represented by R_sc and $L_\mathrm{sc} + L_\mathrm{s}$, whereas R_d and C provide the oscillatory part of the circuit. All the circuit components, except R_sc and L_sc, can be varied over a wide range and with small steps, so that the current and initial few hundred microseconds of the TRV corresponding to the most relevant MV LBS ratings can be obtained [30].

At the start of an interruption test, the test switch is in the closed position. A circuit breaker, CB, at the secondary side of the laboratory transformer closes, so that the current can start to flow through the test circuit. Then, the test switch opens and attempts to interrupt the current. If the test switch fails, i.e., is unable to interrupt the current during the first two or three CZ crossings, the circuit breaker trips and interrupts the current.

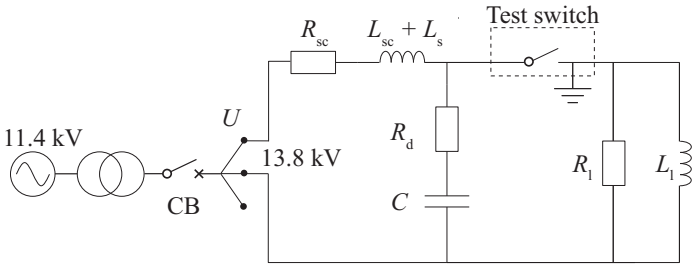

Figure 3.1: The single-phase laboratory test circuit.

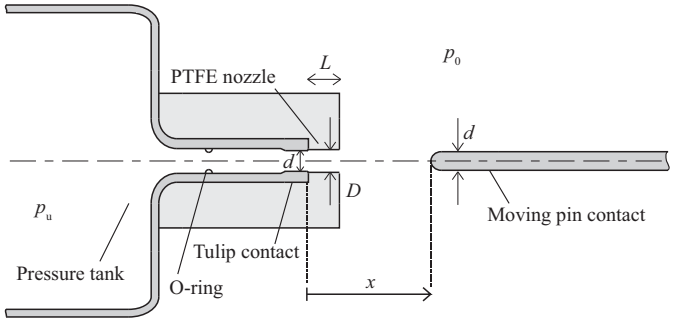

Figure 3.2: The main components of the test switch.

3.2 Test Switch

Fig. 3.2 shows the details of the test switch. A large pressure tank on the left-hand side, which can be pre-set to an upstream over-pressure p_u, is used to provide the cooling air flow during interruption. The surrounding air is at atmospheric pressure, p_0. A tulip contact with inner diameter d is attached to the tank opening, and is one of the two copper-tungsten arcing contacts, together with a moving pin contact (on the right-hand side). A cylindrical PTFE nozzle with inner diameter D and length L guides the air flow onto the electric arc during contact separation. Before an interruption test, the moving pin contact is positioned well inside the tulip contact. Together with an O-ring, it acts as a plug for the tank. When the switch is triggered, a compressed spring pulls the pin contact out of the tank opening, so that the pressurized air in the tank starts flowing out through the tulip contact and nozzle. The pin contact position is denoted by x.

The guiding principle of the test switch is to keep the design as simple as possible, but still be relevant for commercial devices (see, e.g., [19]), with parts that can easily be replaced or changed to different dimensions. In contrast to commercial devices, the air flow is independent of the contact movement, so that the upstream over-pressure in the tank can be changed without increasing the speed of the pin contact. The spring can be released at different times relative to the current waveform, so that the contact position at CZ can be pre-determined and controlled.

Several variables are measured during the interruption tests. The voltage drop across the arcing contacts is measured using a parallel resistive/capacitive voltage divider (500 kΩ/208 pF). A resistive transducer (REGAL KTC375) is used to measure the contact position as a function of time. The pressure sensors used are of the Kistler 4260A type, and the current is measured with a Hall effect current transducer (LEM LT2000-S). All measurements are transmitted through optical fibers to a 12-bit resolution transient recorder at a sampling frequency of 5 MHz.

In addition, a near-infrared high-speed camera (Cheetah 1470 Xeneth) is used during some of the tests to record images of the arc and the surrounding hot gas during the interruption process.

Chapter 4

Interruption Tests and Possible Outcomes

This chapter provides a short step-by-step introduction to the current interruption process, based on some examples obtained from the experimental work. Similar descriptions can be found in textbooks, e.g., [26].

4.1 Contact Separation and Arcing

Although the circuit and test switch parameters are varied for different experimental series, all the interruption tests can be described in a fairly similar manner. Fig. 4.1 shows an example of an interruption test from before contact separation and to the first CZ after separation, with both current and arc voltage measurements, in addition to several high-speed camera images. The images are numbered and the corresponding points on the current and voltage curves are indicated in the plots. The six stages can be described as follows:

1. The pin contact is positioned well inside the tulip contact, providing both good electrical contact and air-tight plugging of the pressure tank. The current flows through the switch, and the voltage drop across the contacts is negligible.

   As indicated by the darkness of the first image, no arc has yet ignited and no hot gas is present.

2. The pin contact starts moving out of the tank opening and the tulip contact. At the point of contact separation, an electric arc is ignited. The current continues to flow in the plasma channel. However, the arc is not as conducting as the metal in the contacts, and the voltage across the contacts starts to increase.

   Some light is now observable through the PTFE nozzle. The pin contact has reached position $x = 0$ mm.

3. The contacts separated not long after the start of a new current half-cycle. As the current increases, the arc grows in size and its temperature rises.

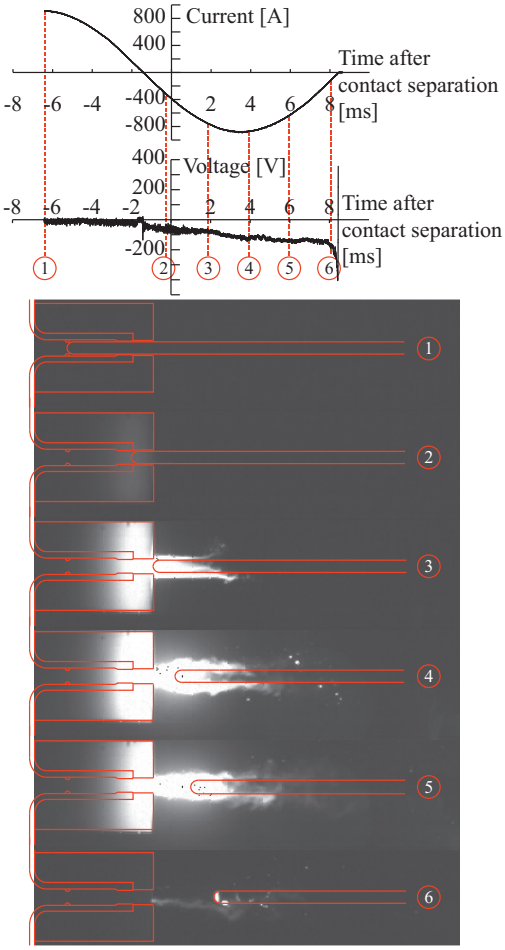

Figure 4.1: An example of the contact opening operation during an interruption test with corresponding current and arc voltage measurements. Both the arc and surrounding hot gas appear bright on the near-infrared images. Contours of the test switch are drawn onto the images.

The arc also heats the surrounding air that has started to flow out of the tulip contact and through the nozzle.

The hot air coming out of the nozzle is now clearly visible, and the light from the arc is also visible through the nozzle walls.

4. At the current peak, the arc is at maximum size and temperature, and more of the surrounding air is heated compared to the previous stage. The arc voltage increases as a function of the arc length, and thus contact gap, and not as a function of the current magnitude.

5. As the current is decreasing, the light emitted from the arc and the hot gas becomes weaker. At the same time, the arc voltage continues to rise with increasing arc length and contact gap.

6. The current eventually approaches its natural CZ. The size and temperature of the arc decrease further, and the electrical conductivity in the plasma channel goes down. This leads to a rapid increase in the arc voltage immediately before CZ.

   In the last image, only a faint light from the arc column can be seen. The tip of the pin contact, which has been heated through the entire current half-cycle, is also visible.

When the arc reaches CZ, there are three possible scenarios. If the air cooling is sufficient and the contact gap is filled with cool air that ensures good dielectric strength, the arc is quenched and the current is successfully interrupted. Failing interruptions can be divided into two categories, namely thermal and dielectric failures. Current interruption is of a stochastic nature, so some interruption tests may succeed and some may fail, given the same conditions. The next sections describe each of these three outcomes in some detail.

4.2 Successful Interruption

Fig. 4.2 presents waveforms and images from a successful interruption. This is the same test as shown in Fig. 4.1. The three stages are described below.

1. The air cooling has been sufficient to extinguish the arc at CZ, and only a thin channel of hot air reveals where the arc was before CZ. Hot particles from the pin and tulip contacts or the nozzle are carried away from the contact gap and downstream of the pin contact by the air flow.

2. After CZ, the current remains zero, whereas the TRV builds up across the contact gap. The tip of the pin contact, where the arc was rooted, is still hot and is clearly visible.

3. Some milliseconds after CZ, the current is still zero and the voltage across the contacts is approaching the system voltage. The pin contact tip has started to cool down.

Obviously, to have a successful interruption, the current should remain zero also beyond the first 2.5 ms shown in Fig. 4.2.

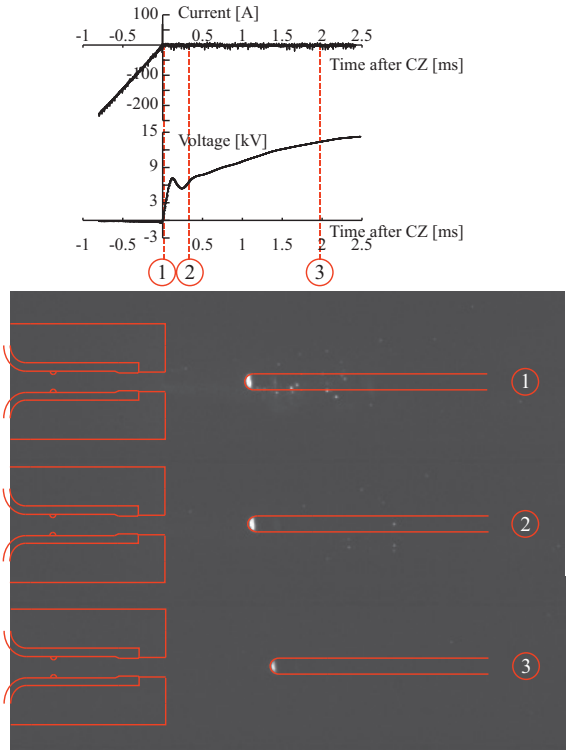

Figure 4.2: A successful interruption with current and voltage measurements, and images of the interruption from CZ and onwards. Contours of the test switch are drawn onto the images.

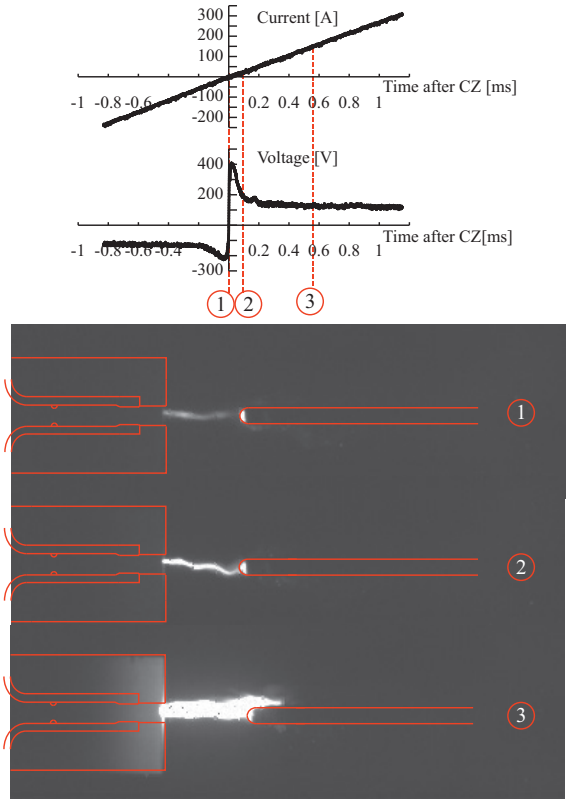

Figure 4.3: Current and voltage measurements, and corresponding images of the test switch and electric arc after a thermal failure.

4.3 Thermal Failure

Immediately after CZ, the contact gap and plasma channel where the arc was burning still contain many charged particles. The channel is hot due to the previous heating from the arc. The larger the current amplitude being interrupted, the more charges in the contact gap. If the air cooling is insufficient, the arc is not quenched and the current will continue to flow until the next natural CZ. This is called thermal failure, and occurs within the first microseconds after CZ, while there are still moving charges in the contact gap, a so-called post-arc current. The steepness of the TRV also determines how difficult the interruption becomes in the thermal phase.

Figure 4.3 shows an interruption attempt suffering thermal failure. As can be seen, the current passes zero without any pause. After the rapid rise in arc voltage before CZ due to increasing resistance of the collapsing arc, the arc voltage changes polarity at CZ. Some microseconds later, the current is high

enough to heat the arc channel, and the arc voltage decreases and stabilizes at approximately 100 – 200 V. The high-speed camera images show that the arc and surrounding hot air channel clearly increase in size from around CZ (1) to 0.55 ms after CZ (3).

4.4 Dielectric Failure

The second type of failed interruption that can occur is referred to as a dielectric failure. After the thermal phase, when the post-arc current has reached zero, the contact gap has started to cool down. Thus, the dielectric strength of the gap increases, and grows as the contact gap becomes larger when the pin contact moves. At the same time, the TRV builds up over the contacts. If the voltage exceeds the dielectric strength of the contact gap a re-strike can occur and a new arc forms. Dielectric re-strikes typically occur milliseconds, not microseconds, after CZ. The larger amplitude of the TRV, the higher the risk of a dielectric failure.

Fig. 4.4 illustrates an example of a dielectric failure. Here, a slightly different nozzle shape was used, with a funnel part at the end of a cylindrical section. The CZ occurred while the pin contact was still inside the nozzle, making it somewhat difficult to observe all details. Still, the main features of a dielectric failure can be identified and described as follows:

1. Similar to the previous cases, no light from the arc is observed at CZ, only some hot particles and gas downstream of the pin contact.

2. As in the case of successful interruption, the current remains zero some time after CZ, and the TRV builds up across the contacts. There is no arc or visible hot gas in the contact gap.

3. At approximately 0.15 ms after CZ, the arc re-strikes. The voltage across the gap drops from more than 6 kV to the typical arc voltage of a few hundred volts. The current curve leaps from zero, and eventually resumes its sinusoidal form towards a new current peak. In the third image, the light from the arc is clearly visible.

The dielectric re-strike in this example occurred 0.15 ms after CZ, and not milliseconds after CZ, which is most common. Only a couple of dielectric re-strikes were observed during the experiments performed in the present work, and the example shown was one of the few that was recorded with the high-speed camera. Thermal failure turned out to be by far the most demanding task in the MV load current interruption tests. Thus, the magnitude of the 50 Hz current and the steepness of the initial part of the TRV determined how difficult the interruptions became, and the amplitude of the recovery voltage several milliseconds later was less important.

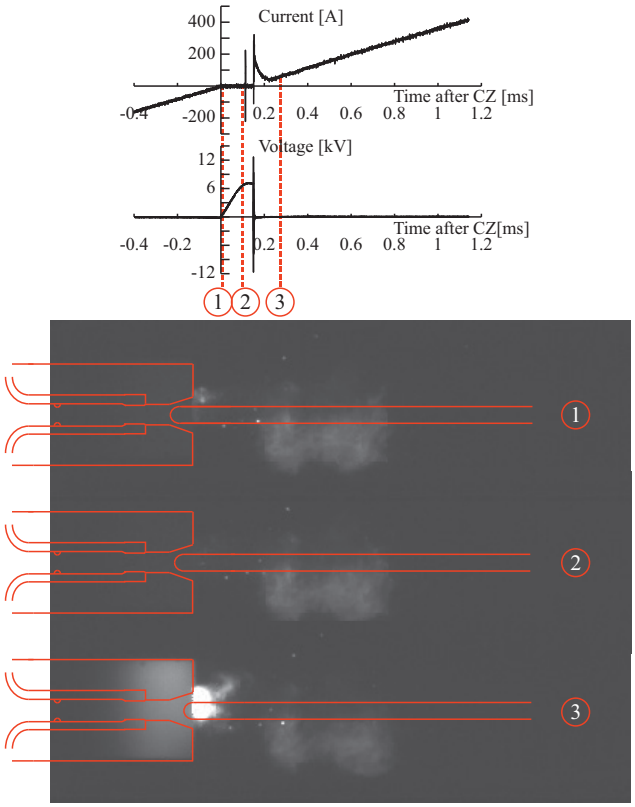

Figure 4.4: A dielectric failure with current and voltage measurements, with corresponding images of the test switch and electric arc.

Chapter 5

Publications

Paper I

Current Interruption in Air for a Medium-Voltage Load Break Switch

Erik Jonsson, Nina Sasaki Aanensen, and Magne Runde
IEEE Transactions on Power Delivery, vol. 29, no. 2, February 2014.

Using a test circuit for 24 kV / 630 A, which is a common LBS rating, and one contact design, the upstream over-pressures needed for successful interruption were found for five different nozzles. Moreover, the pin contact position at CZ was varied to check whether the thermal interruption capability changed with the contact gap.

An over-pressure of approximately 0.3 bar was needed to interrupt the 24 kV / 630 A "mainly active load" test duty as specified in the IEC standard. Interruption performance was found to be far better when the CZ occurred outside the nozzle. The length of the nozzle did not influence the outcome of the interruption tests, but a narrow nozzle was found to require a somewhat lower over-pressure.

Paper II

Air-Flow Investigation for a Medium-Voltage Load Break Switch

Nina Sasaki Aanensen, Erik Jonsson, and Magne Runde
IEEE Transactions on Power Delivery, vol. 30, no. 1, January 2015.

Paper I only considered one contact dimension, and only one current amplitude. The goal of the work presented in this paper was to establish whether the upstream over-pressured needed for successful interruption changed with different contact sizes. By changing the tulip contact inner diameter, the mass flow rate of the cooling air is altered. This could indicate whether it is the pressure of the cooling air, or for example the resulting velocity or mass flow rate that determines the interruption capability.

Three pin and tulip contact sets with different diameters were tested, while keeping the nozzle-to-contact diameter ratio constant. For all three geometries, currents of 400 A, 630 A, and 880 A were tested. The TRV was kept constant.

The experiments showed that the over-pressure needed for successful interruption rose with increasing current, as expected. Moreover, a larger contact diameter required less over-pressure. This suggests that a higher mass flow rate may compensate for reduced upstream over-pressure and air velocity.

Paper III

Empirical Relationships Between Air Load Break Switch Parameters and Interruption Performance

Nina Sasaki Støa-Aanensen, Magne Runde, Erik Jonsson, and Anders Dall'Osso Teigset
Submitted to *IEEE Transactions on Power Delivery*, 2015.

Three parameter studies have been published (Papers I and II, and [32]). The goal of this paper was to consolidate the results and establish empirical relationships between the different test circuit and switch design parameters and the interruption capability. A logistic regression model based on all the obtained experimental results was developed. More than 3 000 interruption attempts formed the input data.

The resulting regression model was able to correctly predict the outcome of approximately 80% of the tests. The model predicted the interruption capability as a function of six test and design parameters, namely the current, the rate of rise of the recovery voltage (RRRV), contact diameter, nozzle-to-contact diameter ratio, nozzle length, and upstream over-pressure. It is considered that the relationships obtained with the idealized test switch will be useful in the design of LBS devices.

Paper IV

Air Flow Measurements During MV Load Current Interruptions

Nina Sasaki Støa-Aanensen and Magne Runde
Accepted to *Symposium on Physics of Switching Arc* and for publication in *Plasma Physics and Technology*, September 2015.

In Paper II, the effect of various air flow rates was investigated by changing the tulip and pin contact diameters. However, the air flow rates and velocities were not measured during the tests, only estimated based on the upstream over-pressure in the tank before contact separation. In this paper a short, but more detailed analysis of the air flow during interruption is presented. The air flow is monitored during the tests by measuring the pressures in a Venturi tube installed between the pressure tank and the tulip contact. With these measurements, the air velocity and mass flow rate can be calculated more precisely. In addition, the influence of the arc on the air flow has been studied.

The typical over-pressures needed for successful load current interruption for MV ratings yield air velocities well below supersonic level. This makes the gas flow in MV load current interruption quite different from that of high voltage circuit breakers. It was also found that the arc clogs the inner part of the nozzle during the high current phase of the half-cycle.

Paper V

Arcing Voltage for a Medium-Voltage Air Load Break Switch

Nina Sasaki Støa-Aanensen, Magne Runde, and Anders Dall'Osso Teigset
Submitted to IEEE Holm Conference on Electrical Contacts, October 2015.

This paper presents an investigation of the arcing voltage before CZ during interruption tests. Thermal interruption is a "race" between the energy transported away by the cooling air and the energy input from the arc. More detailed knowledge about the arc voltage behavior before CZ may give clues about whether the interruption attempt will succeed or not.

A particular issue investigated is the arc voltage close to CZ as a function of contact gap, upstream over-pressure, and current. The measurements showed that the arc voltage behaves as expected, and rises with increasing contact gap, decreasing current, and increasing upstream over-pressure. No differences were found in the arc voltage prior to CZ when comparing successful and failed interruptions.

Paper I

Is not included due to copyright

Paper II

Is not included due to copyright

Paper III

This article has been accepted for publication in a future issue of this journal, but has not been fully edited. Content may change prior to final publication. Citation information: DOI 10.1109/TPWRD.2015.2435804, IEEE Transactions on Power Delivery

Empirical Relationships Between Air Load Break Switch Parameters and Interrupting Performance

Nina Sasaki Støa-Aanensen, Magne Runde, Erik Jonsson, and Anders Dall'Osso Teigset

***Abstract*—A simple gas blow switch consisting of an axisymmetric tulip/pin contact and a cylindrical polytetrafluoroethylene (PTFE) nozzle has been used for empirical studies of medium voltage load current interruption in air. Only the thermal phase of the interruption is considered. Based on the results of more than 3 000 interruption tests, a logistic regression model has been developed to describe the relationships between the switch design and test circuit parameters, and the current interruption capability. The most important design recommendation is that the inner diameter of the nozzle should be only slightly larger than the pin contact. The upstream over-pressure needed for successful interruption increases as a polynomial function of degree 0.5 – 1 with the rate of rise of recovery voltage and of degree 2 – 3 with increasing current.**

***Index Terms*—Load break switch, switchgear, medium voltage, logistic regression, thermal interruption.**

I. Introduction

IN the medium voltage (MV) range, typically 12 – 52 kV, switching equipment less costly than circuit breakers can be applied in many cases. Load break switches (LBS), often in combination with a fuse, are widely used in distribution grids when currents are in the range 400 – 1 250 A. There are two dominating LBS technologies on the market for compact MV switchgear; knife switches, using SF6 as interruption medium and puffer switches, based on SF6 and/or arc quenching materials. In some cases, vacuum interrupters are also used for interrupting load currents. The relatively high cost of vacuum interrupters and the increasing concern about use of so-called "greenhouse gases", have caused the industry to look for new solutions [1] – [3]. One option considered is to replace SF_6 with air. However, the arc quenching and thus the current interruption capability of air is inferior to SF_6, so designing an air-based switch is a far more demanding task. A profound understanding of the interruption process under conditions relevant for MV LBSs is needed to make a compact and cost competitive air switch.

A multitude of factors and parameters must be taken into consideration. The current amplitude and the rate of rise of the recovery voltage (RRRV) across the contacts after interruption determine how difficult the switching duty is. The size and shape of the arcing contacts and nozzle, the contact velocity, and the upstream pressure determine the air flow and are thus crucial for the arc quenching capability.

Previously, several experimental studies on a simple axisymmetric LBS design using air as interrupting medium have been carried out [4] – [6]. One parameter was changed at a time, and simple relations between each parameter (such as current, RRRV and contact diameter) and the required upstream pressure for achieving a successful interruption were established. The outcome of these, and a substantial number of additional interruption tests using the same setup, will in the present work be subjected to a statistical analysis. A technique referred to as logistic regression analysis is applied. The objective is to find a mathematical model, that based on the results (successful or failed interruption) of more than 3 000 tests, estimates in what way and to what extent the various parameters influence the interrupting capability. Some parameters are expected to be more important than others, and it is crucial to identify these and to have some quantitative assessments as to what values they should take in a well-designed air LBS for typical MV ratings. For example, how does interruption capability scale with the nozzle diameter? What upstream pressure is required to successfully interrupt a certain current combined with a certain RRRV?

First, the experimental work serving as input data is briefly reviewed. Second, there is an introduction to logistic regression. The method for selecting regression variables and for evaluating the calculated regression coefficients is then explained. A discussion about what information these analyses provides and how this can be incorporated in the design of MV LBS with air as the interrupting medium, concludes the article.

II. Building a Regression Model

A. Input Data

The contact design and the test circuit parameters used during the experimental work are presented and explained in Figs. 1 and 2, respectively. The approach was to use a contact design that was simple and generic, but not too different from commercial switches. The contacts and nozzles are axisymmetric, and one dimensional parameter can easily be changed at a time. The contacts and nozzles were replaced regularly to avoid effects of erosion and evaporation of nozzle material. The test circuit layout and the selected component values [7] were based on the so-called "mainly active load" test duty specified by the relevant IEC standard for MV LBSs [8].

Three test series using this switch have been reported earlier. The first focused on interruption capability as a function of

This work is supported by the Norwegian Research Council.

N. Sasaki Støa-Aanensen is with the Department of Electrical Power Engineering, Norwegian University of Science and Technology (NTNU), Trondheim 7491, Norway, and with SINTEF Energy Research, Trondheim, 7465, Norway, e-mail: nina.stoa-aanensen@sintef.no.

M. Runde and E. Jonsson are with SINTEF Energy Research, Trondheim 7465, Norway.

A. D. Teigset is with Sweco, Oslo, 0212, Norway.

0885-8977 (c) 2015 IEEE. Personal use is permitted, but republication/redistribution requires IEEE permission. See http://www.ieee.org/publications_standards/publications/rights/index.html for more information.

This article has been accepted for publication in a future issue of this journal, but has not been fully edited. Content may change prior to final publication. Citation information: DOI 10.1109/TPWRD.2015.2435804, IEEE Transactions on Power Delivery

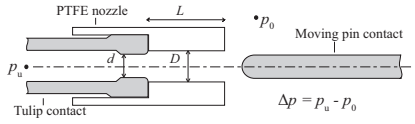

Fig. 1. Geometrical design parameters of the test switch. The tulip and moving pin contacts are both in copper-tungsten. To the left of the tulip contact is a pressure tank which can be pre-set to an upstream over-pressure p_u and drives the air flow onto the arc during contact opening. Consequently, the over-pressure is constant throughout the opening operation, not linked to the contact movement as in puffer devices. At the right hand side of the nozzle the pressure is atmospheric (p_0).

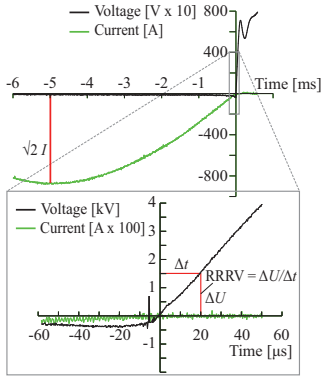

Fig. 2. The current through and voltage over the test switch before and after CZ for a successful interruption. The current frequency is 50 Hz and the amplitude $\sqrt{2}I$. The RRRV is calculated by measuring the voltage 20 μs after CZ.

nozzle length and diameter (L and D) [4]. Tests with five combinations of L and D were carried out while the current, the RRRV and the contact diameter (I, $\dot{U}$ and d) were all kept constant. In the second series, the contact and nozzle geometries were kept constant, while nine combinations of I and $\dot{U}$ were tested [5]. The third series addressed the effect of d, but maintained a constant ratio between the nozzle and contact diameters. Nine combinations of current and contact dimensions were tested [6]. In all three series, the upstream over-pressure for each parameter combination was varied to determine the pressure needed for obtaining 10 out of 10 successful interruptions.

In addition, some 1 350 more interruption tests have been carried out, including experiments with a shorter nozzle, lower nozzle-to-contact diameter ratio (D/d), bringing the total number of interruption tests up to 3 032, covering 43 combinations of test circuits and contact and nozzle designs.

The study is carried out with two important constraints. First, only thermal interruption is considered as this constitutes by far the most demanding part of the current interruption process. Re-strikes occurring several milliseconds after CZ (dielectric re-strikes) are in general of less concern in commercial MV LBSs. Ensuring that the contact gap has a sufficiently large dielectric strength well after the arc has quenched and the gas cooled down is normally fairly straightforward.

The second constraint concerns the contact position at CZs during an interruption test. This position was recorded in all experiments. Similar to commercial devices, the test switch was designed so that at least two CZs occurred during an opening operation. Typically, one of these came while the pin was inside the nozzle, but it was found that the prospects for successful interruption were much better outside the nozzle. The exact position of the pin contact at CZ was not found to matter, as long it occurred outside the nozzle. As a consequence, it was decided to include only the interruption attempts taking place outside the nozzle, and not include the exact contact position as a parameter in the regression model.

Table I lists the parameters measured during the experiments and their value ranges. The nozzle diameter is always greater than the contact diameters, thus the ratio D/d (instead of D alone) is used as a parameter. Essentially, D/d determines the air flow velocity in the nozzle region at a given upstream pressure.

TABLE I
MEASURED PARAMETERS AND BASE FOR REGRESSION MODEL

Parameter	Unit	Range
Upstream over-pressure, Δp	[bar]	[0.05, 1.40]
Current, I	[A]	[300, 900]
RRRV, $\dot{U}$	[V/μs]	[40, 160]
Nozzle length, L	[mm]	[10, 60]
Contact diameter, d	[mm]	[3, 10]
Nozzle-to-contact diameter ratio, D/d		[1.04, 2.67]

The six parameters in Table I are used as a basis for establishing the logistic regression model.

B. Logistic Regression

In multiple regression the outcome is normally a continuous changing value, often expressed by the form:

$$Y(X_1, X_2, ..., X_\mathrm{m}) = \mathrm{b}_0 + \mathrm{b}_1 X_1 + \mathrm{b}_2 X_2 + ... + \mathrm{b}_\mathrm{m} X_\mathrm{m} \quad (1)$$

where the outcome Y is a dependent variable and X_j, j = 1, 2, ..., m are independent variables. Moreover, b_0, ..., b_m are coefficients determined to minimize the difference between the model and the i = 1, ..., n experimental observations.

When making a regression model for the current interruption tests, the independent variables (the Xs) may be taken as the parameters in Table I, or combinations of these (e.g., $I\dot{U}$ or $\Delta p/I$). The outcome, however, is not continuous, but binary, namely successful (1) or failed (0) interruption. Thus, logistic regression should be used, as ordinary multiple regression is unsuited. Here, the independent variables X_1, ..., X_m are used to describe the probability of failed or successful interruption, and the dependent variable (outcome) Y is described by [9]

$$Y = \begin{cases} 1, & P(Y=1) = \pi \\ 0, & P(Y=0) = 1-\pi, \end{cases} \quad (2)$$

stating that π is the probability of Y being 1 and $(1-\pi)$ is the probability of Y being 0.

0885-8977 (c) 2015 IEEE. Personal use is permitted, but republication/redistribution requires IEEE permission. See http://www.ieee.org/publications_standards/publications/rights/index.html for more information.

This article has been accepted for publication in a future issue of this journal, but has not been fully edited. Content may change prior to final publication. Citation information: DOI 10.1109/TPWRD.2015.2435804, IEEE Transactions on Power Delivery

The probability π is defined as

$$\pi = \frac{\exp(\alpha)}{1+\exp(\alpha)} = \frac{\exp(\mathrm{b}_0 + \mathrm{b}_1 X_1 + ... + \mathrm{b}_\mathrm{m} X_\mathrm{m})}{1+\exp(\mathrm{b}_0 + \mathrm{b}_1 X_1 + ... + \mathrm{b}_\mathrm{m} X_\mathrm{m})}. \quad (3)$$

If α is positive and large, $\exp(\alpha)$ becomes even larger, causing the probability of success, π, to approach 1. Similarly, when α is negative and large, π goes towards 0. Furthermore, it can be shown that π has a positive derivative for all values of α, thus the probability of success takes a value between 0 and 1, as it should.

By comparing (1) and (2) – (3), it can be seen that what in multiple regression is defined as the outcome Y is in logistic regression the input α for finding the probability of success.

For the case of π = 0.5, indicating a 50% chance of successful interruption, solving (3) for α yields α = 0. Hence, setting α = 0 can be used to determine for instance how the upstream over-pressure needed for 50% success rate changes with circuit settings or contact design.

When searching for the best regression model, the main tasks are to decide which independent variables X_1, ..., X_m to use and then determine the coefficients b_0, b_1, ..., b_m. Since the independent variables express α and not Y directly, the maximum likelihood estimation will be used to determine the coefficients [9].

The essence of the maximum likelihood estimation method is to find the regression model that gives the highest probability of arriving at the same results as have been observed in the input data (i.e., determining the set of coefficients b_0, ..., b_m giving the highest probability for obtaining the same results as in the experiments). The input data are the n = 3 032 current interruption tests with their experimental parameter values and outcomes (successful or failed interruption). No closed-form solution exists for the b_j's when using the maximum likelihood method.

In this work a commercial software package [10] is used, both to determine the coefficients, calculate the model evaluation indicators, and to search for appropriate independent variable sets. For further reading on logistic regression, see e.g., [9] or [11].

C. Procedure

1) Evaluation Criteria: The ideal situation would be that the regression model correctly predicts the outcome of all the interruption tests. This is, however, not likely as the interruption process itself is stochastic. Repeated test series, each consisting of e.g., 10 interruption tests, carried out under identical conditions are not expected to give exactly the same success ratio every time. Consequently, statistical scatter itself means that it is impossible to establish a model that in all cases predicts whether an interruption is successful or not, at least when a substantial portion of the experiments are carried out under conditions where interruption is barely possible. (If, on the other hand, the experiments were limited to cases where interruption was easy and straightforward and/or virtually impossible, prediction would be easy. However, hardly any new knowledge would be obtained from such an effort.)

The interruption tests were carried out using 43 sets of circuit and switch design parameter combinations. For each combination, the upstream pressure needed for successful interruption was found by carrying out a minimum of 10 interruption tests for at least three pressure levels. As an example, the results of one of these series are presented in Table II.

TABLE II
RESULTS FROM ONE TEST SERIES

Δp [bar]	# successes	# tests	Success ratio
0.2	0	10	0.00
0.3	4	25	0.16
0.4	13	14	0.93
0.5	14	14	1.00

As can be seen, for over-pressures of 0.3 and 0.4 bar both successful and failed interruptions were experienced. Now, define that if the success ratio is 0.50 or higher, the prediction should be 1, and otherwise 0. Applying this to the example in Table II leads to a maximum obtainable prediction precision out of 58 of 63 cases, or 92%. (Four tests at Δp = 0.3 bar succeeded and one test at Δp = 0.4 bar failed.)

Carrying out the same calculation for all 43 parameter combinations leads to a maximum obtainable prediction precision of 87.1%, see Table III. This constitutes the benchmark for any regression model based on the considered data set.

TABLE III
PREDICTED VS OBSERVED SUCCESSES, OVERALL

Predicted	Observed		Prediction presicion
	0	1	
0	1 246	211	87.3%
1	181	1 394	86.9%
Overall			87.1%

At the other end of the scale, predicting that either every interruption attempt fails or succeeds is the simplest prediction model possible. Of the 3 032 interruption tests, 1 427 were failed and 1 605 successful interruptions. Thus, a prediction precision of 53.0% is achieved by simply guessing 1 every time. Consequently, the regression model to be developed should give a prediction precision well above 53.0% and as close as possible to the upper limit of 87.1%.

In addition to the prediction precision, two other model evaluation indicators will be used to assess the quality and credibility of each tested set of independent variables. The first is to check whether the signs of the calculated coefficients b_1, ..., b_m appear physically plausible. For example, if the current interrupted is among the independent variables and the associated coefficient is positive, this is considered clearly non-physical. Increasing the current while keeping all other parameters unchanged, should reduce the chance of having a successful interruption, not increase it. Hence, irrespective of how high the prediction precision becomes, such a particular set of independent variables should not be used.

The other evaluation indicator is the p-value of each coefficient. The p-value is a measure of how important the

0885-8977 (c) 2015 IEEE. Personal use is permitted, but republication/redistribution requires IEEE permission. See http://www.ieee.org/publications_standards/publications/rights/index.html for more information.

This article has been accepted for publication in a future issue of this journal, but has not been fully edited. Content may change prior to final publication. Citation information: DOI 10.1109/TPWRD.2015.2435804, IEEE Transactions on Power Delivery

corresponding independent variable is to the regression model. The p-value essentially indicates the probability of that the coefficient is zero (i.e., that the variable is without importance to the prediction of the outcome) in a particular set of independent variables. The maximum allowed p-value, i.e., the significance level, is set to 0.05, which is a commonly applied limit.

Thus, the various sets of independent variables considered are evaluated according to the following three criteria:

- The coefficients of each independent variable must have a p-value below 0.05.
- The coefficients of each independent variable must have signs that appear physically reasonable.
- The prediction precision should be as high as possible.

The procedure for choosing the set of independent variables is presented next.

2) Independent Variables Selection: An obvious candidate for an independent variable set is the base parameters listed in Table I, giving an expression for α in the form:

$$\alpha_{\mathrm{base}} = \mathrm{b}_0 + \mathrm{b}_1\Delta p + \mathrm{b}_2 I + \mathrm{b}_3\dot{U} + \mathrm{b}_4 L + \mathrm{b}_5 d + \mathrm{b}_6\frac{D}{d}. \quad (4)$$

At first sight, this seems to be a viable and good choice. More careful considerations, however, suggest otherwise. For instance, irrespective of the current amplitude (e.g., 300 A or 900 A) a certain increase of the over-pressure leads to the same increased probability for successful interruption. This is not consistent with the experimental observations, where an increase in pressure of 0.1 bar has a far greater effect on the success rate for low than for high currents. Thus, using independent variables that are combinations of the test circuit and design parameters of Table I may give a better model.

The pool of variables, from which X_1, ..., X_{m} are to be selected, is thus extended to include more complex combinations of the base parameters. To account for the correlated effect of pressure and current on the interruption performance, $\Delta p/I$ and $I/\Delta p$ are added to the pool. In addition, terms linking pressure and RRRV, current and RRRV, and higher degree terms such as I^2 and $\dot{U}^2$ are also included. Moreover, increasing the current leads to a greater arc cross section, and consequently, the current and contact diameter may somehow be linked. To be able to accommodate for this in the model, combinations like I/d or I/d^2 are also included.

Thus, the pool of independent variables considered contains the following candidates: D/d, L, Δp, I, $\dot{U}$, d, $\dot{U}I$, I^2, $\dot{U}^2$, d^2, $\Delta p/I$, $I/\Delta p$, $\Delta p/\dot{U}$, $\dot{U}/\Delta p$, I/d, I/d^2, and $1/d$. This does not imply that all these independent variables should be included in the regression model, but that the search for a set of independent variable here is limited to these variables.

Two methods are used to identify an appropriate set of independent variables; one automatic search function provided by the software used and one manual search procedure. The automatic search sequence starts with no variables (only the constant b_0) and then built-in algorithms evaluate and rate every variable in the pool according to one of three different statistical evaluation methods (referred to as the "Wald", "likelihood ratio" or "conditional" methods [10]). The independent variable obtaining the highest score (i.e., being mostly decisive for whether the interruption is successful or not) is added to the regression model and new coefficients b_0 and b_1 are calculated. This process is then repeated. For every iteration, the independent variables that are already selected are re-evaluated to verify that they are still relevant. If not, they are removed. This iteration process is completed when there are no further improvements found by adding or removing independent variables. The result (i.e., the selected variables, the associated coefficients b_0, ..., b_{m} and p-values) is then checked manually according to the evaluation criteria discussed above. If the result cannot be accepted due to a too high p-value or a non-physical sign of the coefficient, the concerned independent variable(s) is discarded and the automatic search is restarted.

The manual search procedure is significantly more time-consuming than the automatic search function, but is assumed to be a good way to check whether the automatic search function really provides a well optimized regression model. Different independent variable sets are systematically tested to identify the set of independent variables giving the best score based on the p-values, coefficient signs and prediction precision. Table IV lists the variable sets that were tested manually. In addition to the five different pressure terms mentioned earlier, all possible combinations of two of these are included (see column no. 4).

TABLE IV
INDEPENDENT VARIABLE COMBINATIONS

1	2	3	4	5	6	7	8
			Δp				
			$\Delta p/I$				
			$I/\Delta p$				
			$\Delta p/\dot{U}$				
			$\dot{U}/\Delta p$				
			Δp and $\Delta p/I$				
			Δp and $I/\Delta p$	I	$\dot{U}$	d	I/d
D/d	$\dot{U}I$	L	Δp and $\Delta p/\dot{U}$	I^2	$\dot{U}^2$	d^2	I/d^2
	–	–	Δp and $\dot{U}/\Delta p$	–	–	$1/d$	–
			$\Delta p/I$ and $I/\Delta p$			–	
			$\Delta p/I$ and $\Delta p/\dot{U}$				
			$\Delta p/I$ and $\dot{U}/\Delta p$				
			$I/\Delta p$ and $\Delta p/\dot{U}$				
			$I/\Delta p$ and $\dot{U}/\Delta p$				
			$\dot{U}/\Delta p$ and $\Delta p/\dot{U}$				

An independent variable set is formed by selecting one variable from each column in the table. However, for columns containing a "–", selecting no variable is also permitted. This gives a total of $1{\cdot}2{\cdot}2{\cdot}15{\cdot}3{\cdot}3{\cdot}4{\cdot}3 = 6\,480$ independent variable sets. An example of such a set is D/d, L, $\Delta p/I + \Delta p/\dot{U}$ and d. Thus, this gives a regression model without variables from columns no. 2, 5, 6, and 8.

Several of the 6 480 combinations do not contain the current I, and others do not include the contact diameter d or the RRRV $\dot{U}$. Since the experimental results showed that these parameters clearly influence the interruption capability of the switch, they should, in one way or another, be included in the model. Removing combinations not containing all parameters believed to be important (i.e., d, $\dot{U}$, D/d, and I) leaves $5\,442$ sets to be tested manually.

The sets in Table IV do not cover all possible combinations

0885-8977 (c) 2015 IEEE. Personal use is permitted, but republication/redistribution requires IEEE permission. See http://www.ieee.org/publications_standards/publications/rights/index.html for more information.

This article has been accepted for publication in a future issue of this journal, but has not been fully edited. Content may change prior to final publication. Citation information: DOI 10.1109/TPWRD.2015.2435804, IEEE Transactions on Power Delivery

of the independent variables in the pool. However, the combinations included in the assessment are assumed to be relevant considering the experimental results and also sufficient for evaluating the outcome of the automatic search function. More combinations could certainly be added, but presumably yielding only marginal improvements in the model, and with a substantial time cost.

III. Regression Models and Coefficients

A. Base Set of Independent Variables

A model using the base set of independent variables shown in Table I (i.e., the expression for α_{base} in (4)) leads to a prediction precision of 75.6%. The coefficients and corresponding p-values are presented in Table V.

TABLE V
Logistic Regression Model with Base Set

j	Variable	b_j	p-value
0	Constant	9.485	0.000
1	Δp	1.507E+1	0.000
2	I	-7.043E-3	0.000
3	$\dot{U}$	-3.403E-2	0.000
4	L	2.890E-2	0.000
5	d	1.180E-1	0.000
6	D/d	-6.431	0.000

As can be seen, this is an acceptable variable set with regard to both the p-values and the sign of the coefficients. The concern is, as discussed above, that the increase in the interruption success ratio with increasing pressure does not properly reflect the experimental results; the transition from P(success) = 0 to P(success) = 1 when Δp is increased is too slowly. Hence, using the base set of independent variables seems to give somewhat inaccurate predictions.

B. Variable Sets from the Manual and Automatic Searches

Table VI shows the best (i.e., that with the highest prediction precision) independent variable sets found with the manual search procedure, and by using the automatic search function. The prediction precisions are 79.8% and 79.4%, respectively, which is not too far from the benchmark of 87.1%. In addition to having similar prediction precisions, several of the independent variables in the two sets are the same, e.g., the contact and nozzle diameter ratio and the nozzle length. In the base set the pressure, current, RRRV, and contact diameter were independent of each other, whereas in the two new sets they appear in the form $\Delta p/I$, $\dot{U}/\Delta p$, I^2, and either I/d or I/d^2. In addition, the set generated by the automatic search function contains the terms $\Delta p/\dot{U}$ and $\dot{U}$.

Only the best variable set from the manual search is presented here, but all the top five sets (when ranked by their prediction precisions) from this search include D/d, L, $\Delta p/I$, $\dot{U}/\Delta p$ and either I or I^2, as well as I/d or I/d^2. Three of the sets have either $\dot{U}$ or $\dot{U}^2$. This suggests that the independent variables in Table IV that were not included in the best models, such as $\dot{U}I$, d and d^2, are not crucial for describing the outcome of the interruption tests.

TABLE VI
Logistic Regression Model Variable Set, Manual and Auto

j	Variable	Manual search		Automatic search	
		b_j	p-value	b_j	p-value
0	Constant	1.010E+1	0.000	1.021E+1	0.000
1	D/d	-6.419	0.000	-7.479	0.000
2	L	1.340E-2	0.026	1.940E-2	0.005
3	$\Delta p/I$	6.137E+3	0.000	6.654E+3	0.000
4	$\dot{U}/\Delta p$	-8.525E-3	0.000	-5.400E-3	0.000
5	$\Delta p/\dot{U}$			2.671E+2	0.002
6	I^2	-2.189E-6	0.000	-3.211E-6	0.000
7	I/d	-1.361E-2	0.000		
8	I/d^2			-4.644E-2	0.000
9	$\dot{U}$			-1.720E-2	0.000

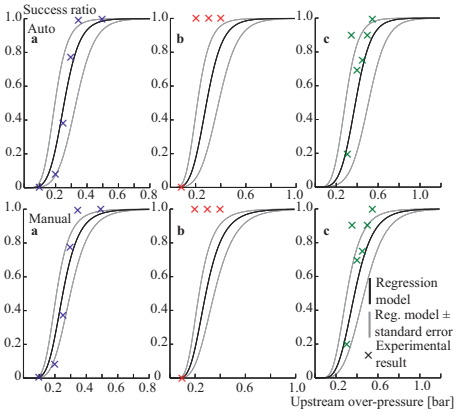

Fig. 3. Comparison of the two regression models and the experimental results of three parameter combinations, **a**, **b** and **c**. In the three upper plots, the model is generated by the automatic search function, and in the lower plots the regression model is found with the manual search procedure.

A top five list from the automatic search is not available, as all three evaluation methods of the software package identified the same variable set. However, looking into the order in which the independent variables are added to the set is of interest. This may indicate the relative importance of the independent variables, based on statistical scores. The order is: $I/\Delta p$ (iteration no. 1), D/d, $\Delta p/I$, $\dot{U}$, I/d^2, $\dot{U}/\Delta p$, I^2, $\Delta p/\dot{U}$, $I/\Delta p$ removed, L (iteration no. 10). Hence, the variables D/d and $\Delta p/I$ appear more important than $\Delta p/\dot{U}$ and L.

In Fig. 3, experimental results from three of the 43 tested parameter combinations are presented together with the regression model from the automatic (upper part) and the manual (lower part) search procedures. The first, **a**, represents what is considered a good fit between models and experiments. The second, **b**, is an example of a poor fit. The two regression models are based on the input data from all the 43 different parameter combinations, and are thus expected to reveal the major trends of the entire test program. Inevitably, for some parameter combinations the models are unable to accurately fit the experimental results.

0885-8977 (c) 2015 IEEE. Personal use is permitted, but republication/redistribution requires IEEE permission. See http://www.ieee.org/publications_standards/publications/rights/index.html for more information.

This article has been accepted for publication in a future issue of this journal, but has not been fully edited. Content may change prior to final publication. Citation information: DOI 10.1109/TPWRD.2015.2435804, IEEE Transactions on Power Delivery

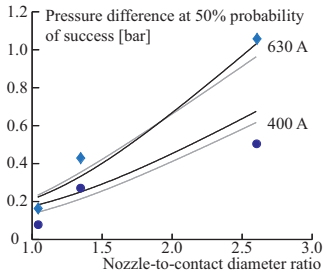

Fig. 4. The upstream over-pressure required to obtain a 50% interruption success ratio as a function of the nozzle-to-contact diameter ratio for 400 and 630 A. The black and gray lines represent the manual and automatic regression models, respectively. The symbols are estimated $\Delta p_{50\%}$-values from the experiments. Here, d = 4 mm, $\dot{U}$ = 73 V/μs and L = 12 mm, except for the experimental values at D/d = 2.6, where L = 30 mm.

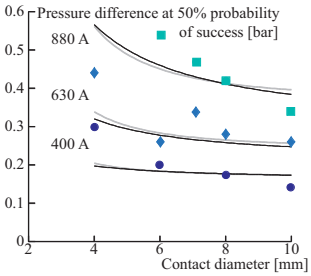

Fig. 5. $\Delta p_{50\%}$ as a function of the contact diameter at three different currents. The black and gray lines represent the manual and automatic regression models, respectively. The symbols are estimated $\Delta p_{50\%}$-values from the experiments. Here, D/d = 1.35, $\dot{U}$ = 73 V/μs and L = 30 mm, except the two points to the left (d = 4 mm), where L = 12 mm.

Part **c** shows a case where the experimental results are difficult to interpret, because the success ratio is not consistently increasing with increased pressure, as is normally expected. This is assumed to be statistical scatter caused by the stochastic nature of current interruption. Obviously, obtaining a good fit to experimental results with simple regression models is not possible in such cases.

The next section contains a thorough examination of the experimental results and the regression models, by considering one parameter at a time. The main objective is to determine how the various design and circuit parameters affect the interrupting performance of the switch.

IV. Switch Design and Circuit Parameters

A. Nozzle Length, L

According to Table VI, increasing the length of the nozzle increases the probability of success somewhat. For example, in the case of d = 6.1 mm, D/d = 1.5, $\dot{U}$ = 71 V/μs and I = 630 A, increasing the nozzle length from 15 to 60 mm reduces the upstream over-pressure needed to obtain a 50% probability of success, $\Delta p_{50\%}$, from 0.34 bar (0.33 bar) to 0.30 bar (0.30 bar) according to the regression model from the automatic (manual) search.

Consequently, the nozzle length does not seem to be a crucial parameter during thermal interruption for an MV LBS operating in air. The corresponding p-values for L are comparatively large, see Table VI, supporting this assertion.

B. Nozzle-to-Contact Diameter Ratio, D/d

Fig. 4 shows the pressure difference needed for 50% probability of success as a function of the nozzle-to-contact diameter ratio for 400 and 630 A. Both models fit the experimental results reasonably well.

Obviously, $\Delta p_{50\%}$ depends heavily on the nozzle-to-contact diameter ratio. For the current of 630 A, increasing the ratio from 1.05 to 2.6 increases the required upstream over-pressure from around 0.2 bar to around 1.0 bar.

As described earlier, the expressions for $\Delta p_{50\%}$ from the two regression models are derived by setting $\alpha = 0$ and solving for $\Delta p_{50\%}$. For each model, this expression contains all the independent variables and their coefficients. In order to assess how the various test circuit and switch design parameters affect the current interruption capability, $\Delta p_{50\%}$ can be expressed solely as a function of one parameter at a time, while keeping the remaining parameters constant. Using this approach for the nozzle-to-contact diameter ratio, $\Delta p_{50\%}(D/d)$ is for both regression models

$$\Delta p_{50\%}\left(\frac{D}{d}\right) = \mathrm{a_0}^* + \mathrm{a_1}\frac{D}{d} + \sqrt{\mathrm{a_2}\left(\frac{D}{d}\right)^2 + \mathrm{a_3}^*\left(\frac{D}{d}\right) + \mathrm{a_4}^*}. \quad (5)$$

The constants $\mathrm{a_0}$, $\mathrm{a_1}$, ..., $\mathrm{a_4}$ contain the coefficients $\mathrm{b_0}$, ..., $\mathrm{b_m}$ and all parameters except D/d, and are different for the two regression models. Constants that take both positive and negative values (dependent on the circuit and design parameters), are marked by an asterisk (*). The others are always positive.

Eq. (5) shows that the interruption capability increases as a polynomial function of degree one with the nozzle-to-contact diameter ratio. This is consistent with the experimental results shown in Fig. 4.

C. Contact Diameter, d

Fig. 5 shows $\Delta p_{50\%}$ as a function of d for three different currents. Both the regression models and the experimental results suggest that increasing the size of the contact diameter decreases the required upstream pressure needed for successful interruption. There are, however, deviations between the two models and the experimental results, especially for smaller contact diameters.

The expressions for $\Delta p_{50\%}$ as a function of the contact diameter become

$$\Delta p_{50\%\mathrm{a}}(d) = \mathrm{c_0}^* + \mathrm{c_1}\frac{1}{d^2} + \sqrt{\mathrm{c_2}\frac{1}{d^4} + \mathrm{c_3}^*\frac{1}{d^2} + \mathrm{c_4}^*}, \quad (6)$$

$$\Delta p_{50\%\mathrm{m}}(d) = \mathrm{d_0}^* + \mathrm{d_1}\frac{1}{d} + \sqrt{\mathrm{d_2}\frac{1}{d^2} + \mathrm{d_3}^*\frac{1}{d} + \mathrm{d_4}^*}, \quad (7)$$

0885-8977 (c) 2015 IEEE. Personal use is permitted, but republication/redistribution requires IEEE permission. See http://www.ieee.org/publications_standards/publications/rights/index.html for more information.

This article has been accepted for publication in a future issue of this journal, but has not been fully edited. Content may change prior to final publication. Citation information: DOI 10.1109/TPWRD.2015.2435804, IEEE Transactions on Power Delivery

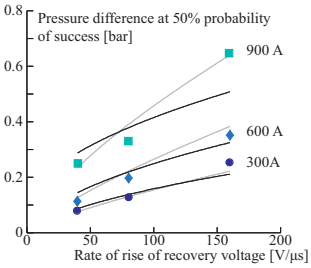

Fig. 6. $\Delta p_{50\%}$ as a function of the RRRV at three different currents. The black and gray lines represent the manual and automatic regression models, respectively. The symbols are estimated $\Delta p_{50\%}$-values from the experiments. Here, d = 6.1 mm, D/d = 1.15 and L = 20 mm.

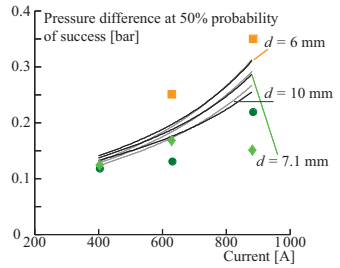

Fig. 7. $\Delta p_{50\%}$ as a function of the current with three different contact diameters. The black and gray lines represent the manual and automatic regression models, respectively. The symbols are estimated $\Delta p_{50\%}$-values from the experiments. Here, D/d = 1.04, $\dot{U}$ = 73 V/μs and L = 12 mm, except the points d = 6 mm, where L = 10 mm.

where $\Delta p_{50\%\mathrm{m}}$ and $\Delta p_{50\%\mathrm{a}}$ refer to the manually and automatically obtained models, respectively. The d-dependency in the two regression models is not the same, since one model has I/d^2 as one of the independent variables and the other I/d, see Table VI. Despite this difference, the two models give similar predictions for the cases in Fig. 5.

D. Rate of Rise of Recovery Voltage, $\dot{U}$

In Fig. 6, $\Delta p_{50\%}$ is plotted as a function of the RRRV for three currents. As expected, the pressure required for successful interruption rises with increasing RRRV, approximately by a factor 3 when the RRRV increases from 40 to 160 V/μs. The model found by the automatic search function gives the following relationship between $\dot{U}$ and $\Delta p_{50\%}$:

$$\Delta p_{50\%\mathrm{a}}(\dot{U}) = \frac{\dot{U}\left[(\mathrm{e}_0\dot{U} + \mathrm{e}_1{}^*) + \sqrt{\mathrm{e}_2\dot{U}^2 + \mathrm{e}_3{}^*\dot{U} + \mathrm{e}_4{}^*}\right]}{(\mathrm{e}_5\dot{U} + \mathrm{e}_6)}. \tag{8}$$

Hence, $\Delta p_{50\%}$ increases as a polynomial function of degree one with $\dot{U}$.

The expression for $\Delta p_{50\%\mathrm{m}}(\dot{U})$ derived from the manual search, however, shows a square root relationship:

$$\Delta p_{50\%\mathrm{m}}(\dot{U}) = \mathrm{f}_0{}^* + \sqrt{\mathrm{f}_1\dot{U} + \mathrm{f}_2}. \tag{9}$$

For the nine experimental results in Fig. 6, the model from the automatic search fits better than the model from the manual search, in particular at 900 A.

Furthermore, Fig. 6 shows that the increase in $\Delta p_{50\%}$ is smaller when increasing the current from 300 to 600 A, than from 600 to 900 A (in both cases a 300 A rise). This suggests a current dependency of a degree higher than one.

E. Current, I

As seen in Table VI, both models include three independent variables containing the current. Moreover, the model from the automatic search has an extra Δp-term compared to the model from the manual search. This leads to different $\Delta p_{50\%}(I)$ expressions:

$$\Delta p_{50\%\mathrm{a}}(I) = \frac{I\left(\mathrm{g}_0{}^* + \mathrm{g}_1 I^2 + \mathrm{g}_2 I\right)}{\mathrm{g}_9 + \mathrm{g}_{10} I} + \frac{1}{\mathrm{g}_9 + \mathrm{g}_{10} I} \cdot \cdot\sqrt{I\left(\mathrm{g}_3 I^5 + \mathrm{g}_4 I^4 + \mathrm{g}_5{}^* I^3 + \mathrm{g}_6{}^* I^2 + \mathrm{g}_7{}^* I + \mathrm{g}_8\right)}, \tag{10}$$

$$\Delta p_{50\%\mathrm{m}}(I) = I\left(\mathrm{h}_0{}^* + \mathrm{h}_1 I + \mathrm{h}_2 I^2\right) + + \sqrt{I\left(\mathrm{h}_3 I^5 + \mathrm{h}_4 I^4 + \mathrm{h}_5{}^* I^3 + \mathrm{h}_6{}^* I^2 + \mathrm{h}_7{}^* I + \mathrm{h}_8\right)}. \tag{11}$$

The models suggest a I-dependency of the second and third degrees, respectively.

Fig. 7 shows how the pressure estimates $\Delta p_{50\%\mathrm{m}}$ and $\Delta p_{50\%\mathrm{a}}$ vary with current for three contact diameters. The two regression models give similar curves, but fit the experimental results poorly. Changing the contact diameter in the experiments significantly changes the pressure needed to successfully interrupt. The regression models predict less variation in $\Delta p_{50\%}(d)$, similar to what was observed in Fig. 5. The pressure needed for successful interruption appears to be underestimated for small contact diameters and somewhat overestimated for larger contacts.

The d = 7.1 mm / I = 880 A experimental value is puzzling. (This is the same parameter combination used as an example of a poor fit in Fig. 3.) To be in line with the rest of the results, a $\Delta p_{50\%}$ closer to 0.3 bar rather than 0.15 bar would be expected.

V. Discussion

A. Regression Model

The highest obtainable prediction precision for the particular set of experimental results is 87.1%, whereas the two regression models scored 79.4% (automatic) and 79.8% (manual). One reason for this gap, as discussed in Section II-C, is the stochastic nature of the current interruption process itself. Even with as many as 3 032 interruption tests, statistical scatter remains an important factor due to the high number of parameters involved.

Only six circuit and design parameters are used in the regression models. This is a fairly simple way to describe the complicated process of current interruption. Including more

0885-8977 (c) 2015 IEEE. Personal use is permitted, but republication/redistribution requires IEEE permission. See http://www.ieee.org/publications_standards/publications/rights/index.html for more information.

This article has been accepted for publication in a future issue of this journal, but has not been fully edited. Content may change prior to final publication. Citation information: DOI 10.1109/TPWRD.2015.2435804, IEEE Transactions on Power Delivery

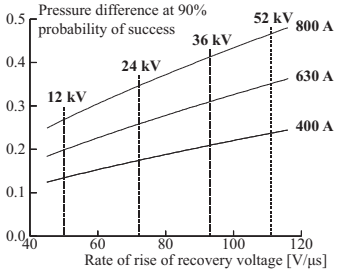

Fig. 8. Upstream over-pressure needed for 90% probability of success for d = 10 mm, D/d = 1.04 and L = 20 mm at various current and voltage classes (in bold), calculated from the logistic regression model found by the automatic search function. The current ratings and the RRRV values are according to the "mainly active load" test duties of the IEC standard [8], [7].

complex parameters (e.g., air velocity or cooling power) may possibly lead to more accurate predictions. However, the six parameters used in this work are all readily available and also relevant to most switches employing forced gas cooling of the arc.

Taking these matters into account, the two regression models are assumed to reasonably identify the main relationships between switch design and interrupting capability under different conditions.

The regression model obtained using the automatic search function appears as good as, or even slightly better than the model from the manual search. The automatic search is substantially faster, and in the present investigation is found to be the better option.

B. Optimizing Switch Design

According to the regression model coefficients, the nozzle length is not important for the interruption capability, although a long nozzle is somewhat more beneficial than a short one. However, as discussed in Section II-A, the interruption capability is poorer when the pin contact is inside the nozzle at CZ. The longer the nozzle, the higher is the risk of having the first CZ occurring with the pin contact inside the nozzle, giving fewer CZs and interruption attempts at the outside.

With regard to the pin/tulip contact size, a large diameter requires a lower upstream over-pressure for successful interruption, especially when the current is large. This is reasonable, as a larger tulip inner diameter allows for a higher air flow rate. However, in a puffer switch design, a larger contact diameter implies a larger puffer volume. Thus, the choice of contact diameter is a trade-off between low upstream pressure and large puffer volume.

Irrespective of the contact diameter, a low nozzle-to-contact diameter ratio is essential. Thus, the nozzle inner diameter should be only slightly larger than the pin contact. This is probably the most important design recommendation from this study.

Figure 8 shows an example of how an optimized MV air switch (large d, small D/d) is expected to perform with different currents and RRRVs. Here, $\Delta p_{90\%}$ is used instead of the $\Delta p_{50\%}$. The figure indicates that with an upstream over-pressure of approximately 0.5 bar, currents up to 800 A can be interrupted in all MV classes. Moreover, the figure also suggests that, when only considering thermal interruption, a 12 kV / 630 A switch can be applied at 36 kV, when de-rated to 400 A. In order to maintain the current rating of 630 A, the upstream over-pressure during interruption must be increased from around 0.2 to 0.3 bar.

The examples above only deal with the thermal phase of the current interruption. Other type test duties, such as closing operation against a short-circuit, and dielectric withstand test, must of course also be considered when developing switchgear.

VI. Conclusions

A logistic regression analysis of 3 032 interruption tests in atmospheric air using an idealized MV test switch has been carried out for load currents of 300 – 900 A, and with RRRVs in the range 40 – 160 V/μs. The main conclusions regarding the switch design are:

- A low nozzle-to-contact diameter ratio is favorable in terms of requiring less upstream over-pressure for successful interruption.
- A large contact diameter is beneficial, but requires a larger puffer volume.
- The upstream over-pressure needed for successful interruption increases with $\dot{U}^{\beta}$ and I^{γ} and, where $0.5 < \beta < 1$ and $2 < \gamma < 3$.

The study is limited to the thermal phase of the current interruption process.

Acknowledgment

The authors gratefully acknowledge the contributions from John Tyssedal and Magne Saxegaard.

References

[1] A. Morita, "Recent Topics of the Medium-Voltage Switchgear in Japan", *IEEE T/D Conference*, Yokohama, pp. 1450–1454, 2002.
[2] J. H. Lee, J. S. Ryu, H. W. Joo, S. J. Tak, S. W. Park, and J. H. Lee, "Insulation Characteristics of Various Conditions for Eco-friendly High Voltage Switchgear", *Int. Conf. on Elect. Mach.*, Rome, 2010.
[3] C. M. Franck, D. A. Dahl, M. Rabie, P. Haefliger, and M. Koch, "An Efficient Procedure to Identify and Quantify New Molecules for Insulating Gas Mixtures", *Cont. to Plasma Phys.*, vol. 54, no. 1, pp. 3–13, 2014.
[4] E. Jonsson, N. S. Aanensen, and M. Runde, "Current interruption in air for a medium voltage load break switch", *IEEE Trans. Power Del.*, vol. 29, no. 2, pp. 870–875, 2014.
[5] E. Jonsson and M. Runde, "Current interruption in air for medium voltage load break switch ratings", *IEEE Trans. Power Del.*, vol. 30, no. 1, pp. 161 – 166, 2015.
[6] N. S. Aanensen, E. Jonsson, and M. Runde, "Air Flow Investigation for a Medium Voltage Load Break Switch", *IEEE Trans. Power Del.*, vol. 30, no. 1, pp. 299 – 306, 2015.
[7] E. Jonsson and M. Runde, "Medium voltage laboratory for load break switch development", the *Proc. Int. Conf. Power Systems Transients*, Vancouver, 2013.
[8] *High-voltage switchgear and controlgear - Part 103: Switches for rated voltage above 1 kV up to and including 52 kV*, IEC International Standard no. 62 271-103, ed 1.0, 2011.
[9] M. H. Kutner, C. J. Nachtsheim, J. Neter, W. Li, "Applied Linear Statistical Models", fifth edition, McGraw-Hill Irwin, 2005.
[10] IBM Corp. Released 2012, IBM SPSS Statistics for Windows, version 21.0 Armonk, NY: IBM Corp.
[11] D. W. Howmer and S. Lemeshow, "Applied Logistic Regression", third edition, John Wiley & Sons, New York, 2013.

0885-8977 (c) 2015 IEEE. Personal use is permitted, but republication/redistribution requires IEEE permission. See http://www.ieee.org/publications_standards/publications/rights/index.html for more information.

Paper IV

Is not included due to copyright

Paper V

Arcing Voltage for a Medium-Voltage Air Load Break Switch

Nina Støa-Aanensen
Norwegian Univ. of Science and Technol.
Trondheim 7491, Norway,
and
SINTEF Energy Research
Trondheim 7465, Norway
E-mail: nina.stoa-aanensen@sintef.no

Magne Runde
SINTEF Energy Research
Trondheim 7465, Norway

Anders Dall'Osso Teigset
Sweco
Oslo 0212, Norway

***Abstract*—Air is an environmentally benign and attractive alternative to SF_6 as arc quenching gas in switching devices for modest current and voltage ratings. Several interruption tests with a simple air medium-voltage load break test switch have been carried out to investigate the arc and the arcing voltage behavior for different circuit and switch design parameters. During the first half-cycle after contact separation, the arc voltage is typically 100 – 200 V. Approximately 50 μs before current zero the arc voltage increases in magnitude, before collapsing at current zero. The arc voltage increases with increasing contact gap, with decreasing current, and with increasing air flow. The arc voltage measurements from this work are believed to be suitable as experimental reference for verifying results from computational current interruption models.**

***Index Terms*—Load break switch, switchgear, medium voltage, arc, arc voltage, thermal interruption.**

I. Introduction

SF_6-free technology is becoming increasingly attractive for the medium voltage (MV) switchgear market, as reducing the use of SF_6 will in the long term also lower the emissions of this strong "greenhouse gas" to the atmosphere. Vacuum technology is an obvious option today, but for load current interruption with moderate voltage transients, there may be less costly alternatives. In particular, a compact air based load break switch (LBS) is considered an interesting solution for use in metal encapsulated (metal clad) switchgear for the large 12 - 36 kV market.

A LBS for such modest ratings may be a fairly simple, axisymmetric design, with a pin-tulip contact, a polytetrafluoroethylene (PTFE) nozzle and arrangements for blowing gas onto the arc. Previous investigations examined how the various design features (contact and nozzle geometries, air flow) of a simple, generic air LBS affected its interrupting capability under different conditions (current amplitude, steepness of recovery voltage) [1] – [4]. A substantial number of interruption tests were carried out, and the studies were limited to the critical thermal part of the current interruption, i.e., the first tens of microseconds after current zero (CZ). (Avoiding dielectric re-ignitions and re-strikes is less of a problem in MV LBSs.)

The present work examines the arc and the arcing voltage behavior during current interruption using this simple switch. Several parameters such as current amplitude, gas blow, contact position at CZ, nozzle design, etc. are varied in a systematic manner. The objective is to clarify how these parameters affect the arc characteristics, in particular the arc voltage.

The arc voltage is an essential output from computational models of current interruption. When designing switching equipment, such models are widely used as a complement to empirical studies and laboratory testing. For large high-voltage SF_6 circuit breakers sophisticated numerical models have proven a useful design tool. For MV LBSs using air at much lower pressures and velocities, matters become very different and computational models for this application are still in their infancy.

The main purpose with the work reported on here is to provide experimental data that can be used for developing and verifying numerical models for current interruption under conditions and ratings relevant for MV LBSs based on air. In particular, measurements of the arcing voltage immediately before CZ are believed to be important. A few high-speed camera images of the arc at various stages of an interruption process are also included to visualize the arc behavior and for interpreting the recorded arcing voltage traces.

II. Experimental Setup

The test switch design is shown in Fig. 1. The arcing contact pair is a tulip/pin design with diameter d and is made of copper-tungsten. A cylindrical PTFE nozzle with length L and inner diameter D is fixed to the tulip contact and guides the air flow onto the arc.

The tulip contact is connected to a large pressure tank, which can be pre-set to an upstream over-pressure $p_u > p_0$, and provides air flow during interruption tests. The moving pin contact acts as a plug for the tank before contact separation. During an interruption test, the pin contact is pulled out of the tulip at a speed of approximately 5 m/s, by releasing a compressed spring. The position of the moving pin contact, relative to the tulip is denoted by x.

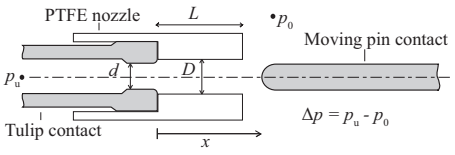

Fig. 1. The axisymmetric test switch. To the left of the tulip contact is a pressure tank which can be pre-set to an upstream over-pressure p_u and drives the air flow onto the arc during contact opening. At the right hand side of the nozzle the pressure is atmospheric (p_0).

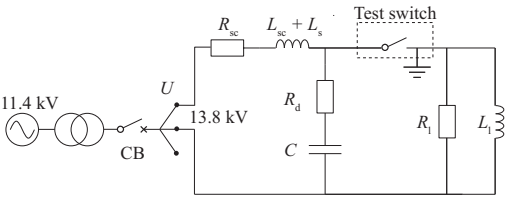

Fig. 2. The circuit used for the interruption tests. The circuit is a single-phase version of the "mainly active load" test duty type test of the LBS standard issued by IEC [5]. The system voltage is 13.8 kV at 50 Hz.

The idea behind the test switch design is that it should provide switching conditions similar to those of typical commercial devices, while keeping the setup as simple as possible. Parameters such as current, transient recovery voltage, contact position at CZ, upstream over-pressure, and switch design characteristics can be changed independently. In this way, the effect of each design parameter on the interruption performance, including the arcing voltage, can be examined.

Fig. 2 shows the test circuit. The arc voltage is measured with a parallel resistive/capacitive voltage divider and transmitted through optical fiber to a 12-bit resolution transient recorder. The sampling frequency is 5 MHz, and a five-sample running average has been applied to smoothen the output. The accuracy of the voltage measurement is approximately 30 V.

A near-infrared high-speed camera (Cheetah 1470, Xeneth) has been used to capture images of the arc during interruptions. The integration time is 3.7 μs with a resolution of 384×120 pixels, giving a recording rate of approximately 10 870 frames per second. In addition to the arc voltage measurement and image recordings, the current and the contact position are measured during the interruption tests.

For further information about the laboratory setup and test circuit settings see [6] and [3].

III. General Arc Voltage Considerations

It is usually found that the voltage across arcs burning in a gas (i.e., not vacuum arcs) to the first approximation increases linearly with the length of the arc,

$$U_{\mathrm{arc}}(l) = U_{\mathrm{anode}} + U_{\mathrm{cathode}} + \mathrm{C}l, \qquad (1)$$

where U_{anode} and U_{cathode} are the voltage drops at the electrodes or contacts, and l is the length of the arc. The constant C depends on a number of factors, including gas type, pressure and cooling conditions.

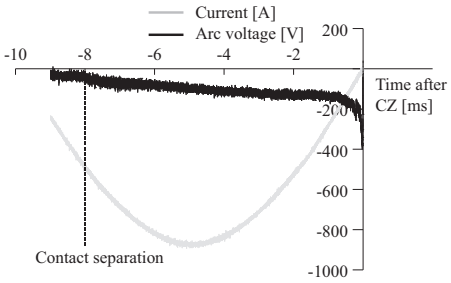

Fig. 3. Arc voltage and current measurement from contact separation and until current interruption. The current is 630 A / 50 Hz.

For arcs burning in still air, C is in the range 1 – 2 V/mm for currents between 100 and 20 000 A [7] – [9]. Moreover, it has been found that the voltage drop at the electrodes, $U_{\mathrm{anode}} + U_{\mathrm{cathode}}$, is almost constant in the same current range [10], and around 15 – 20 V.

For lower currents, the arc voltage increases with decreasing current. Forced cooling also tend to increase the arc voltage, as the electrical conductivity of the plasma is highly dependent on its temperature.

Fig. 3 shows a typical example of current and arc voltage measurements from contact separation and until CZ and extinction, obtained with the setup described above. As can be seen, the arc voltage amplitude increases from approximately 100 to 200 V in the high current region. This increase is presumably caused by the arc becoming longer during the pin contact movement. The arc voltage makes up only a few percent of the system voltage.

As the current decreases towards CZ, the amplitude of the arc voltage rises to around 400 V. This initiates the critical part of the current interruption process. A low current means a smaller arc which is less stable and more vulnerable to the forced air cooling. The phenomena taking place in the short time intervals (tens of microseconds) before and after CZ are decisive for whether the current is interrupted, or a thermal re-ignition occurs.

The next sections concentrate on the arc voltage behavior immediately before CZ and how it changes with different parameters, such as contact gap, air over-pressure, and current.

IV. Arc Voltage Measurements

A. Arc Voltage vs. Contact Gap at CZ

Fig. 4 shows the arc voltage just before CZ for interruption tests with different contact gaps at CZ. All other parameters are kept constant. As expected, the cases where the contact gap is larger at CZ yield higher arc voltages. In all tests, the arc voltage collapses towards zero within the last 10 – 20 μs before CZ.

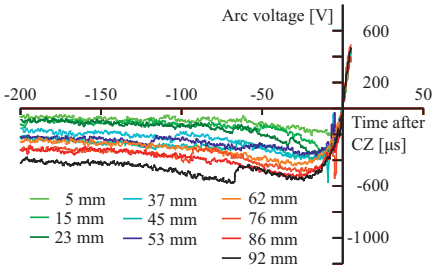

Fig. 4. Measured arc voltage the last 200 μs before CZ for different arcing contact gaps. In these interruption tests, d = 7.1 mm, D = 9.6 mm, L = 30 mm, I = 630 A, and Δp = 0.30 bar. The rate of rise of the recovery voltage is 73 V/μs.

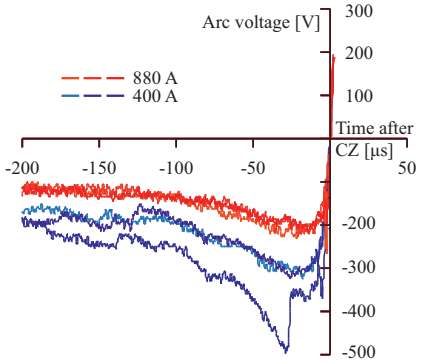

Fig. 5. Measured arc voltage around CZ for 400 and 880 A. In these interruption tests d = 7.1 mm, D = 7.4 mm, L = 12 mm, and Δp = 0.2 bar. The rate of rise of the recovery voltage is 73 V/μs. The pin contact position x is between 28 and 34 mm at CZ.

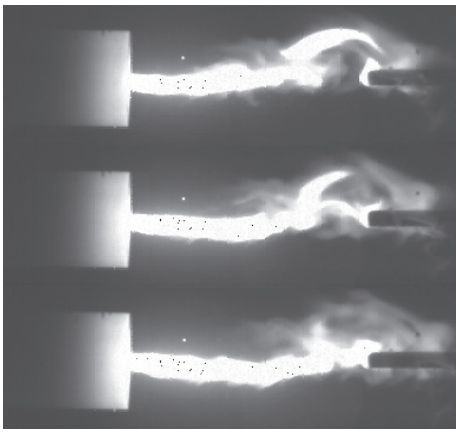

Fig. 6. A "short-circuiting" of a part of an arc channel. The arc finds a new and shorter way from the tulip to the pin contact, causing a sudden arc voltage drop as seen in one of the 400 A tests of Fig. 5. Here, the current is 630 A. The "short-circuiting" occurred approximately 2 ms after a CZ, and the time between each frame is approximately 92 μs. The arc voltage dropped from approximately 400 to 320 V.

With basis in the arc voltage values measured at current peak (at -5 ms, not included in Fig. 4), the constant C in (1) can be estimated. (The three tests with contact distances of 5, 15, and 23 mm are not included in this calculation, as the current peak here came before contact separation.) The resulting C value is 2.6 V/mm, which is somewhat higher than found in [7] – [9]. The difference may at least partly be explained by that the contact gap is used as a measure of the arc length, which may underestimate its length. Moreover, the arcs are here not burning in still air, but subjected to forced cooling.

At -200 μs the current is approximately 56 A. The measurements shown in Fig. 4 can also be used to estimate the value of C, this time in the region where the arc voltage is expected to increase with decreasing current. The calculated values of C at -200 μs (56 A) and -50μs (14 A) become 3.5 V/mm and 4.4 V/mm, respectively.

B. Arc Voltage vs. Current Amplitude

Fig. 5 shows the arc voltage before CZ from six interruption tests with two different currents, 400 and 880 A. The arc voltages for the three 880-A experiments are similar and increase from around 120 V at -200 μs to a maximum of approximately 200 V just before CZ. The arc voltages for the 400 A tests are higher, with a maximum of more than 300 V. One of the latter three curves shows significantly larger voltage values than the other two, with clear signs of "short-circuiting" of a part of the arc approximately 30 μs before CZ. A sudden reduction in arc length is accompanied by a steep drop in the arc voltage amplitude. Fig. 6 shows an image sequence of such a phenomenon.

The difference between the 400 and 880 A arc voltage curves can be attributed to two factors. First, in the time interval shown in Fig. 5, the current is below 100 A for both cases, i.e., in a region where a small current results in a higher arc voltage than with a larger current. Second, the rate of the change of the current, $\mathrm{d}I/\mathrm{d}t$, is different in the two cases. The arc voltage depends on the electric conductivity and other material properties of the arc medium. Even though the properties may change rapidly, there are some inertia involved causing a certain response time, typically in the microsecond range. With a rapidly decreasing current the arc voltage may not be able to respond sufficiently fast. Consequently, the arc voltage of the 880-A case has a significantly lower peak value before it collapses at CZ than in the 400-A case.

C. Arc Voltage vs. Upstream Over-Pressure

This section investigates to what extent the arc voltage changes with the upstream over-pressure, i.e., the air flow and cooling of the arc. Reducing the temperature of the arc plasma

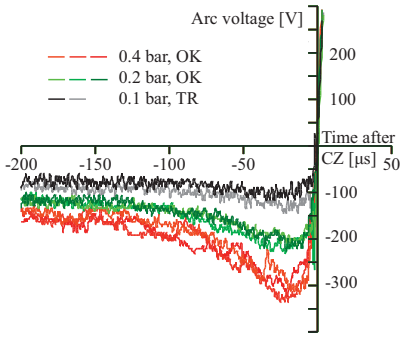

Fig. 7. Measured arc voltage before CZ for different upstream over-pressures. In these tests d = 7 mm, D = 7.4 mm, L = 12 mm, and I = 880 A. The rate of rise of the recovery voltage was 73 V/μs. All interruption attempts occurred with the pin contact position x between 29 and 34 mm at CZ. At 0.1 bar over-pressure, both interruption attempts failed, with a thermal re-strike (TR). The other tests interrupted successfully (OK).

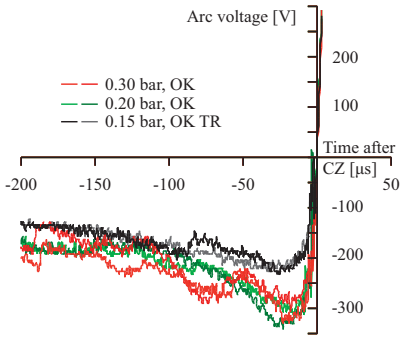

Fig. 8. Measured arc voltage before CZ for different upstream over-pressures. In these interruption tests d = 7.1 mm, D = 7.4 mm, L = 12 mm, and I = 630 A. The rate of rise of recovery voltage was 73 V/μs. All interruption attempts occurred with the pin contact position x between 35 and 37 mm at CZ. At 0.15 bar over-pressure, one interruption attempt failed and one succeeded. The other interruption tests were successful.

increases its resistance and leads to a higher arc voltage. Consequently, an increased air over-pressure is expected to give a higher arc voltage, especially near CZ.

Fig. 7 shows the arc voltage development before CZ as a function of the upstream over-pressure for a 880-A current. Increasing the over-pressure in the range 0.1 – 0.4 bar clearly causes a higher arc voltage. This difference is especially apparent from -50 μs and onwards, with a voltage peak of around 100 V for 0.1 bar compared to 300 V for the 0.4 bar tests.

Furthermore, the shape of the arc voltage curves in Fig. 7 differs somewhat. A higher upstream pressure causes a more pronounced voltage increase before CZ, and a less smooth arc voltage curve. This suggests that the air flow interacts strongly with the arc, providing better cooling. The 0.2 and 0.4 bar experiments were successful interruptions, whereas the 0.1 bar tests suffered thermal re-ignition.

In Figs. 8 and 9 similar arc voltage measurements for 630 A and 400 A are shown. The same trends and observations as discussed for Fig. 7 are also seen here. A higher upstream pressure leads to more forceful cooling, higher and more fluctuating voltage, and better prospects for a successful interruption.

Fig. 10 shows high-speed camera images comparing two arcs and the surrounding hot air with and without forced air cooling. Both these interruption attempts failed. There is a striking difference between the two cases. Without forced cooling, the hot air and plasma channel is much thicker, and appears brighter. A jet of hot gas seems to stream out from the nozzle and flow past the pin contact tip. With forced cooling, there is far less hot and ”glowing” air surrounding the arc.

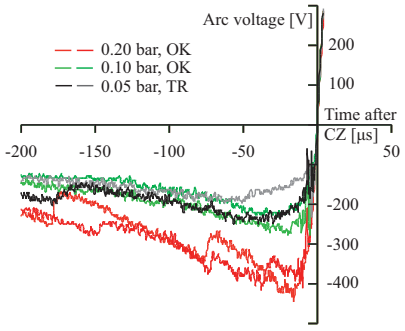

Fig. 9. Measured arc voltage around CZ for different upstream over-pressures. In these interruption tests d = 10 mm, D = 10.4 mm, L = 12 mm, and I = 400 A. The rate of rise of the recovery voltage was 73 V/μs. All interruption attempts occurred with the pin contact position x between 30 and 35 mm at CZ. The two interruption tests at 0.05 bar over-pressure failed, whereas the others were successful.

D. Arc Voltage vs. Shape of Nozzle

In addition to the cylindrical-shaped nozzles that have been used in the interruption tests shown so far, some experiments using a cylindrical nozzle with a funnel-shaped end part (see Fig. 11) were carried out.

Figs. 12 and 13 show the arc voltages obtained with the two nozzle types for upstream over-pressures of 0.15 and 0.20 bar, respectively. The arc voltage is somewhat lower when using the funnel-shaped nozzle. The interrupting capability, however, was found to be the same in the two cases.

It is not clear why there is a small difference in the arc voltage in the two cases. One possibility is that the nozzle changes the air flow around the arc, and thus the arc cooling.

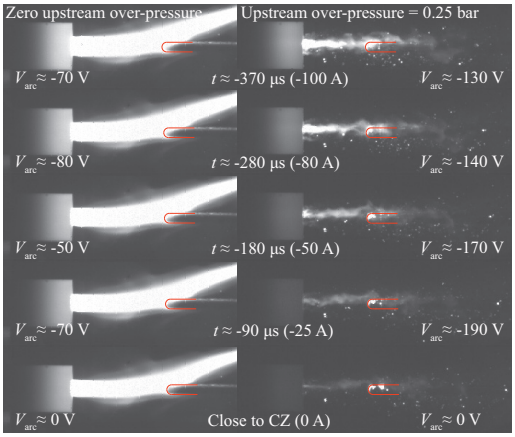

Fig. 10. High speed camera images of two different arcs and surrounding hot air before CZ, one without forced air cooling and one with an upstream over-pressure of 0.25 bar. The current is 630 A. The approximate times before CZ and corresponding current and arc voltage values are given for each image. The contour of the pin contact is drawn onto the images.

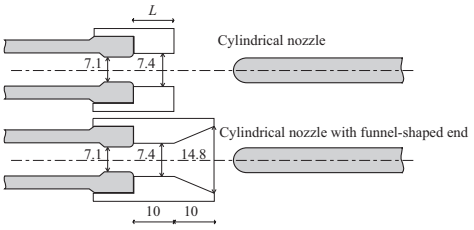

Fig. 11. The two different nozzle shapes used in the interruption tests discussed in Section IV-D. Dimensions are in millimeter.

Irrespective of the cause of the difference in arc voltage, this is an example of a situation where a higher arc voltage does not necessarily imply an increased probability for a successful interruption, as is the case when reducing the current or increasing the upstream over-pressure.

Fig. 14 shows typical examples of the arc with the two different nozzle designs. The upper images are at approximately 1.1 ms before CZ, and the bottom images show the arc close to CZ. Both were failed interruptions.

There are no obvious differences in the shape and intensity of the arc and hot air between these two nozzle designs. Whether forced air cooling was applied or not, as shown in Fig. 10, gave a far greater change in the appearance of the arc.

E. Arc Voltage; Failed vs. Successful Interruption

An interesting question is if the arc voltage just before CZ can provide clues as to whether the interruption fails or succeeds. This would be particularly important when using simulation tools to develop new switchgear design.

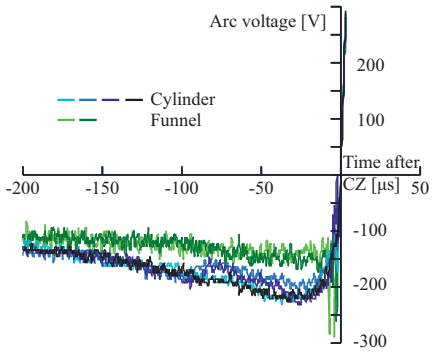

Fig. 12. Measured arc voltage around CZ for two different nozzles, one cylindrical and one with a funnel section. In these interruption tests, d = 7.1 mm, D = 7.4 mm, L = 12 mm (cylindrical nozzle), I = 630 A, and Δp = 0.15 bar. The rate of rise of the recovery voltage was 73 V/μs. All interruption attempts occurred with the pin contact position x between 31 and 37 mm at CZ. All attempts shown here failed.

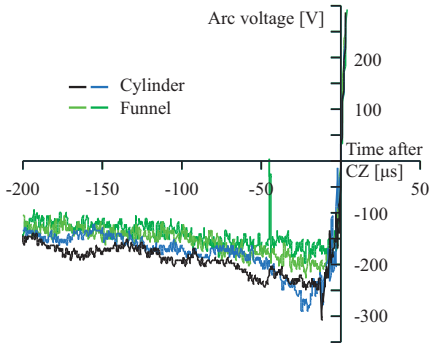

Fig. 13. Measured arc voltage around CZ for two different nozzles, one cylindrical and one with a funnel section. In these interruption tests, d = 7.1 mm, D = 7.4 mm, L = 15 mm (cylindrical nozzle), I = 630 A, and Δp = 0.20 bar. The rate of rise of the recovery voltage was 73 V/μs. All interruption attempts occurred with the pin contact position x between 33 and 39 mm at CZ, and lead to successful interruptions.

In Fig. 15, six arc voltage measurements are presented, of which three were from successful and three from failed interruption attempts. All tests were performed with a pin contact position of 18 mm at CZ, which is inside the nozzle. The upstream over-pressure was 0.3 bar, a pressure level giving approximately 50% successful interruptions.

As can be seen, there are only minor variations among the measurements. Additional experiments with the pin contact positioned at 17 and 19 mm at CZ did not reveal any further clues. Hence, predicting the outcome of the interruption attempt based on the arc voltage characteristics just before CZ was not possible.

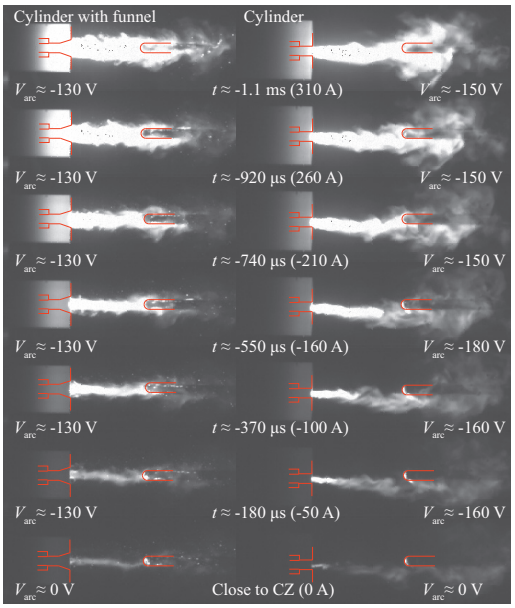

Fig. 14. High-speed camera images of two different arcs and surrounding hot air around CZ, one with a cylindrical nozzle (right column) and one with a nozzle that is half cylindrical and half funnel-shaped (left column). The current is 630 A, and the upstream over-pressure is 0.15 bar. The approximate times before CZ and corresponding current and arc voltage values are given for each image. The contours of the pin contact and inner part of the tulip contact and nozzle are drawn onto the images.

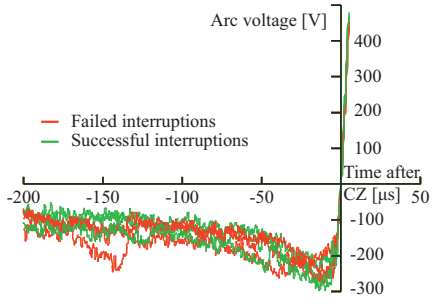

Fig. 15. Measured arc voltage around CZ for three successful and three failed interruptions. In these interruption tests, d = 7 mm, D = 9.6 mm, L = 30 mm, and I = 630 A. The rate of rise of the recovery voltage was 73 V/μs. All interruption attempts occurred with the pin contact position x = 18 mm at CZ.

A combination of arc voltage and current measurement, including the small post arc current some microseconds after CZ, may be required to get a more detailed understanding of the arc behavior. However, obtaining accurate measurements (and also modeling) of the post arc current, which is two or three orders of magnitude smaller than the load current, is difficult.

V. Conclusions

Several interruption tests for a simple MV load break test switch using air as cooling gas have been carried out to investigate how the arc voltage before CZ varies with different circuit and switch design parameters. The main conclusions are:

- During the first half-cycle after contact separation, the arc voltage is typically 100 – 200 V.
- Approximately 50 μs before CZ the arc voltage increases in magnitude, before collapsing at CZ.
- The arc voltage before CZ increases with the contact gap (approximately 4 $\pm$ 0.5 V/mm), with decreasing current, and with increasing upstream over-pressure.
- When comparing arc voltages just before CZ for failed and successful interruptions, no differences were observed in the arc voltage characteristics.

The arc voltage measurements from this work are believed to be suitable for use as experimental reference when verifying results from computational simulation models.

Acknowledgments

This work is supported by the Norwegian Research Council.

References

[1] E. Jonsson, N. S. Aanensen, and M. Runde, "Current interruption in air for a medium voltage load break switch", *IEEE Trans. Power Del.*, vol. 29, no. 2, pp. 870–875, 2014.

[2] E. Jonsson and M. Runde, "Current interruption in air for medium voltage load break switch ratings", *IEEE Trans. Power Del.*, vol. 30, no. 1, pp. 161 – 166, 2015.

[3] N. S. Aanensen, E. Jonsson, and M. Runde, "Air Flow Investigation for a Medium Voltage Load Break Switch", *IEEE Trans. Power Del.*, vol. 30, no. 1, pp. 299 – 306, 2015.

[4] N. S. Støa-Aanensen, M. Runde, E. Jonsson, and A. D. Teigset, "Emipirical relationships between load break switch parameters and interrupting performance", submitted to *IEEE Trans. Power Delivery*, 2015.

[5] *High-voltage switchgear and controlgear - Part 103: Switches for rated voltage above 1 kV up to and including 52 kV*, IEC International Standard no. 62 271-103, ed 1.0, 2011.

[6] E. Jonsson and M. Runde, "Medium voltage laboratory for load break switch development", the *Proc. Int. Conf. Power Systems Transients*, Vancouver, 2013.

[7] V.V. Terzija and H. J. Koglin, "Testing, modeling and simulation of long arcs in still air", *Power Engineering Society Winter Meeting*, IEEE, vol. 3, 2001.

[8] R. Smeets, L. van der Sluis, M. Kapetanovic, D. Peelo, and A. Janssen, "Switching in Electrical Transmission and Distribution Systems", Wiley, 2015.

[9] A. P. Strom, "Long 60-Cycle Arcs in Air", *AIEE Transactions*, vol. 65, 1946.

[10] Y. Yokomizu, T. Matsumura, R. Henmi, and Y. Kito, "Total voltage drops in electrode fall regions of SF_6, argon and air arcs in current range from 10 to 20 000 A", *J. Phys. D: Applied Physics*, vol. 29, pp. 1260 – 1267, 1996.

Chapter 6

Discussion and Conclusions

LBS Design Parameters

Three papers concern switch design parameters that could be of importance when optimizing an air LBS for use in compact devices. The tulip/pin arcing contact pair and PTFE nozzle used were similar to those found in commercial devices. The test circuit provided currents and voltage transients that are typical for MV ratings, and according to the single-phase version of the "mainly active load" test duty as issued by IEC [35].

It was found that the pin contact position at CZ was not important for the interruption capability, as long as the pin contact tip was outside of the nozzle. The length of the nozzle did not seem to have an impact on the breaker performance, either, except that there is a higher chance of having a CZ while the pin contact is still inside the nozzle if the nozzle is long. Moreover, the nozzle should not be too short, as this allows the arc to bend away from the cooling air flow.

The nozzle diameter turned out to be extremely important for the interruption capability. A narrow nozzle compared to the pin and tulip contact diameter, i.e., a low nozzle-to-contact diameter ratio, requires a far lower upstream air over-pressure than when using a wide nozzle. This is an inexpensive and effective way to optimize an existing switch design, as it improves the interruption capability without requiring more space or a more powerful driving mechanism.

The choice of pin/tulip contact diameter also affected the ability of the breaker to interrupt the current. The required upstream over-pressure for successful thermal interruption is slightly reduced when increasing the tulip contact inner diameter. Thus, it is probable that an increased mass flow rate can compensate for a slightly reduced over-pressure and air velocity.

The air cooling was provided by filling a large pressure tank connected to the tulip contact to a predetermined upstream over-pressure. By carrying out several interruption tests at different pressure levels, the over-pressure necessary for successful interruption was found. Commercial switches, however, typically use a puffer device that is driven by the contact movement to generate the gas flow. This volume is much smaller than what is used in the present work, so not all the results concerning the air flow properties and air flow / arc influence are directly transferable from this experimental work to a commercial design. For

example, an increased mass flow rate due to a larger tulip contact will require a larger puffer volume to ensure that the air flow lasts for the same period of time as when using a smaller tulip contact. The air flow must be maintained for at least one and a half half-cycles after contact separation to ensure successful interruption for all three phases.

Three main test circuit settings were used to provide three different current and voltage combinations relevant for the 24 kV LBSs. The values of the 50 Hz currents were 400 A, 630 A and 880 A, respectively. In addition, experimental results from [32] with a wider range of currents and TRVs were used as input to make a logistic regression model. The model suggests that the upstream over-pressure required for interrupting the current successfully increases proportionally to

$$\dot{U}^{\beta}, \qquad 0.5 < \beta < 1 \tag{6.1}$$

and

$$I^{\gamma}, \qquad 2 < \gamma < 3, \tag{6.2}$$

where $\dot{U}$ is the initial steepness of the TRV (the RRRV) and I is the current. The tested ranges of the currents and RRRV were [300 A, 900 A] and [40 V/μs, 160 V/μs].

Arc Influence on Air Flow and Arc Voltage

Two of the papers investigated the details of the current interruption process, namely the arc / air flow interaction and the arc voltage before CZ. Based on pressure measurements recorded during interruption tests, it was found that the arc clogs the inside of the tulip contact and nozzle during the high current part of the half-cycle, even at relatively low currents and with large tulip contact inner diameters. This means that the arc itself affects the air flow during current interruption, and this must be taken into account when designing and optimizing puffer devices for MV LBSs. Furthermore, it was found that the typical upstream over-pressures needed for successful interruption corresponds to air velocities well below supersonic level.

The arc voltage is typically less than 200 V during the first half-cycle after contact separation. When approaching CZ, the arc voltage increases rapidly, before collapsing at CZ and changing polarity. At low currents, the arc voltage rises with decreasing current. Moreover, the arc voltage increases as a function of increasing contact gap and increasing upstream over-pressure. There is a clear, visible difference between cases with and without forced cooling of the arc and surrounding hot gas when comparing images taken by a near-infrared high-speed camera. No significant difference was observed in the arc voltage between successful and failed interruptions.

Suggestions for Further Work

Thermal interruption is a race between the energy input from the circuit to the arc and the cooling of the arc by the air flow. A brief investigation into the details of the arc voltage around CZ has been made, but without obtaining sufficient information to predict the outcome of an interruption attempt. In the present work, the current measurements were not accurate enough to examine the current waveform just before CZ, or to measure the post-arc current in

the microseconds after CZ. Such measurements are believed to be important for better understanding of the details involved in the thermal phase of the interruption. A suggestion is to perform such measurements in the future, even though it is complicated to accurately measure currents of several orders less in magnitude than the load current.

As mentioned above, a pressure tank was used instead of a puffer device. This was done to make the contact movement independent of the air flow, so that the effect of each parameter could be studied separately. Important information about the over-pressures required for interrupting different currents with different test switch designs were obtained, in addition to certain details about the corresponding air velocity and mass flow rate.

The next natural step would be to perform interruption tests using a test switch with an air blowing mechanism that is more similar to the commercial devices, namely a puffer arrangement. Based on the already gained knowledge from the simple test switch with the pressure tank, more detailed recommendations directly applicable for designing commercial LBSs could be established.

Furthermore, other type test requirements than the "mainly active load" test duty exist, such as tests for LBS / fuse combinations. These have steeper TRVs and also higher voltage peaks. Consequently, the dielectric phase of the current interruption may be relevant for some of the other duties that LBSs may experience.

Nozzle material investigations have not been a part of this work. Nozzles made of PTFE were used in all experiments and are known to be quite inert. The use of more "active" materials, so-called ablation materials, may be of interest in future LBSs, and have shown promising effects on the current interruption capability [33], [34]. This field should be investigated further, by proposing nozzle designs that are optimized for ablation, not air flow.

The last suggestion for further work is to bring theory closer to the experimental results by developing numerical models for the current interruption process. Such models exist for higher voltage SF_6 circuit breakers, but are not directly transferable to MV ratings, load currents, and air. The test switch has a very simple axisymmetric design, with a contact movement that is independent of the air flow. This setup is far easier to implement in computational models than most commercial devices, with more complex parts and an interlinked contact/piston movement. By developing multi-physics models that are able to reproduce the results seen in the experiments, a more complete understanding of the current interruption process could be obtained than what is possible to achieve through empirical investigations alone.

References

[1] J. F. Perkins and L. S. Frost, "Effect of nozzle parameters on SF_6 arc interruption", the *IEEE PES Summer Meeting*, pp. 961 – 970, San Francisco, 1972.

[2] G. Frind and J. A. Rich, "Recovery speed of axial flow gas blast interrupter: dependence on pressure and dI/dt for Air and SF_6", the *IEEE PES Winter Meeting*, pp. 1675 – 1684, New York, 1973.

[3] J. J. Lowke and H. C. Ludwig, "A simple model for high-current arcs stabilized by forced convection", *J. Applied Physics*, vol. 46, no. 8, pp. 3352 – 3360, 1975.

[4] G. R. Jones, D. Lidgate, and H. Edels, "Interaction between a high-current arc and the air flow in an air-blast circuit breaker", in *proc. Instit. Electrical Engineers*, vol. 122, no. 12, pp. 1443 – 1451, 1975.

[5] W. Hermann, U. Kogelschatz, L. Niemeyer, K. Ragaller, and E. Schade, "Investigation on the physical phenomena around current zero in HV gas blast breakers", *IEEE Trans. Power Apparatus and Systems*, vol. PAS-95, no. 4, pp. 1165 – 1176, 1976.

[6] W. Hermann and K. Ragaller, "Theroretical description of the current interruption in HV gas blast breakers", *IEEE Trans. Power Apparatus and Systems*, vol. PAS-96, no. 5, pp. 1546 – 1555, 1977.

[7] S. Ramakrishnan, T. P. Dang, D. Chadwick, and J. F. Armstrong, "An experimental study of circuit-breaker arcs in nozzles under clogged conditions", *IEEE Trans. Plasma Science*, vol PS-10, no. 4, pp. 331 – 338, 1982.

[8] C. M. Franck and M. Seeger, "Application of high current and current zero simulations of high-voltage circuit breakers", *Contrib. Plasma Phys.*, vol. 46, no. 10, pp. 787 – 797, 2006.

[9] N. P. Basse, M. M. Abrahamsson, M. Seeger, and T. Votteler, "Quantitative analysis of gas circuit breaker physics through direct comparison of 3-D simulations to experiment", *IEEE Trans. Plasma Science*, vol. 36, no. 5, pp. 2566 – 2572, 2008.

[10] N. P. T. Basse, R. Bini, and M. Seeger, "Measured turbulent mixing in a small-scale circuit breaker model", *OSA Applied Optics*, vol. 48, no. 32, pp. 6381 – 6391, 2009.

[11] R. Bini, N. T. Basse, and M. Seeger, "Arc-induced turbulent mixing in an SF_6 circuit breaker model", *J. Phys. D: Applied Physics*, vol. 44, 2011.

[12] J. D. Yan, K. I. Nuttall, and M. T. C. Fang, "A comparative study of turbulence models for SF_6 arcs in a supersonic nozzle", *J. Phys. D: Applied Physics*, vol. 32, pp. 1401 – 1406, 1999.

[13] J. L. Zhang, J. D. Yan, and M. T. C. Fang, "Investigation of the effects of pressure ratios on arc behavior in a supersonic nozzle", *IEEE Trans. Plasma Science*, vol. 28, no. 5, pp. 1725 – 1734, 2000.

[14] Q. Zhang, J. D. Yan, and M. T. C. Fang, "Current zero behaviour of an SF_6 nozzle arc under shock conditions", *J. Phys. D: Applied Physics*, vol. 46, 2013.

[15] M. Claessens, R. von Starck, and H. G. Thiel, "Simulations of gas flow phenomena in high-voltage self-blast circuit breakers at heavy fault current interruption", *IEEE Trans. Plasma Science*, vol. 25, no. 5, pp. 1001 – 1007, 1997.

[16] P. H. Schavemaker and L. van der Sluis, "An improved Mayr-type arc model based on current-zero measurement", *IEEE Trans. Power Delivery*, vol. 15, no. 2, pp. 580 – 584, 2000.

[17] N. Osawa and Y. Yoshioka, "Calculation of transient puffer pressure rise takes mechanical compression, nozzle ablation, and arc energy into consideration", *IEEE Trans. Power Delivery*, vol. 20, no. 1, pp. 143 – 148, 2005.

[18] N. Osawa, Y. Yoshioka, "Effect of puffer volume and operating force on dielectric recovery performance in thermal puffer-type gas circuit breaker", *IEEE Trans. Power Delivery*, vol. 20, no. 3, pp. 1897 – 1903, 2005.

[19] E. Attar, P. Stoller, M. Schwinne, P. Skryten, N. Ranjan, B. Wuethrich, T. R. Bjørtuft, O. Granhaug, "Gas flow analysis in low energy arc puffer interrupters", the *22nd Int. Conf. Electricity Distribution*, Stockholm, 2013.

[20] A. Morita, "Recent topics of the medium-voltage switchgear in Japan", in *Transmission Distr. Conf. Exhibition* vol. 2, pp. 1450 – 1454, 2002.

[21] P. C. Stoller, M. Seeger, A. A. Iordanidis, and G. V. Naidis, "CO_2 as an arc interruption medium in gas circuit breakers", *IEEE Trans. Plasma Science*, vol. 41, no. 8, pp. 2359 – 2369, 2013.

[22] Y. Yokomizu, R. Ochiai, and T. Matsumura, "Electrical and thermal conductivities of high-temperature CO_2-CF_3I mixture and transient conductance of residual arc during its extinction process", *J. Phys. D: Appl. Phys*, vol. 42, no. 21, 2009.

[23] J. D. Mantilla, N. Gariboldi, and S. Grob, M. Claesens, "Investigation of the insulation performance of a new gas mixture with extremely low GWP", in *Elect. Ins. Conf.*, pp. 469 – 473, Philadelphia, 2014.

[24] M. Rabie and C. M. Franck, "Predicting the electric strength of proposed SF_6 replacement gases by means of density functional theory", the *18th Int. Symp. High Voltage Engineering*, pp. 1381 – 1386, Seoul, 2013.

[25] T. Rokunohe, Y. Yagihashi, K. Aoyagi, T. Oomori, and F. Endo, "Development of SF_6-free 70.5 kV GIS", *IEEE Trans. Power Delivery*, vol. 22, no. 3, pp. 1869 – 1876, 2007.

[26] R. Smeets, L. van der Sluis, M. Kapetanovic, D. Peelo, and A. Janssen, "Switching in Electrical Transmission and Distribution Systems", Wiley, 2015.

[27] S. Stewart, "Distribution switchgear", The Institution of Engineering and Technology, 2nd edition, 2008.

[28] R. W. Johnson, "The Handbook of Fluid Dynamics", CRC Press, 1998.

[29] E. Jonsson, "Load current interruption in air for medium voltage ratings", PhD Thesis, Norwegian University of Science and Technology, Department of Electric Power Engineering, Trondheim, 2014.

[30] E. Jonsson and M. Runde, "Medium voltage laboratory for load break switch development", the *Proc. Int. Conf. Power Systems Transients*, Vancouver, 2013.

[31] E. Jonsson, N. S. Aanensen, and M. Runde, "Current interruption in air for a medium-voltage load break switch", *IEEE Trans. Power Delivery*, vol. 29, no. 2, pp. 870 – 875, 2014.

[32] E. Jonsson and M. Runde, "Interruption in air for different medium-voltage switching duties", *IEEE Trans. Power delivery*, vol. 30, no. 1, pp. 161 – 166, 2015.

[33] E. Jonsson, M. Runde, G. Dominguez, A. Friberg, and E. Johansson, "Comparative study of arc-quenching capabilities of different ablation materials", *IEEE Trans. Power Delivery*, vol. 28, no. 4, 2013.

[34] G. Gjendal, E. Jonsson, and M. Runde, "Ablation assisted current interruption in a medium voltage load break switch", the *Proc. Int. Conf. Electrical Contacts*, Dresden, 2014.

[35] *High-voltage switchgear and controlgear - Part 103: Switches for rated voltage above 1 kV up to and including 52 kV*, IEC International Standard no. 62 271-103, ed 1.0, 2011.